

Elliptical Attention

Stefan K. Nielsen^{◇,*} Laziz U. Abdullaev^{†,*} Rachel Teo[†] Tan M. Nguyen[†]

National University of Singapore[†]

FPT Software AI Center[◇]

June 21, 2024

Abstract

Pairwise dot-product self-attention is key to the success of transformers that achieve state-of-the-art performance across a variety of applications in language and vision. This dot-product self-attention computes attention weights among the input tokens using Euclidean distance, which makes the model prone to representation collapse and vulnerable to contaminated samples. In this paper, we propose using a Mahalanobis distance metric for computing the attention weights to stretch the underlying feature space in directions of high contextual relevance. In particular, we define a hyper-ellipsoidal neighborhood around each query to increase the attention weights of the tokens lying in the contextually important directions. We term this novel class of attention Elliptical Attention. Our Elliptical Attention provides two benefits: 1) reducing representation collapse, and 2) enhancing the model’s robustness as the Elliptical Attention pays more attention to contextually relevant information, rather than focusing on some small subset of informative features. We empirically demonstrate the advantages of Elliptical Attention over the baseline dot-product attention and state-of-the-art attention methods on various practical tasks, including object classification, image segmentation, and language modeling across different data modalities.

1 Introduction

Attention mechanisms and transformers [71] have achieved state of the art performance across a wide variety of tasks in machine learning [22, 30, 66] and, in particular, within natural language processing [1, 2, 10, 56, 9], computer vision [13, 34, 68, 57, 53], and reinforcement learning [20, 4]. They have also demonstrated strong performance in knowledge transfer from pretraining tasks to various downstream tasks with weak or no supervision [54, 55, 12]. At the core of these models is the dot-product self-attention mechanism, which learns self-alignment between tokens in an input sequence by estimating the relative importance of each token with respect to all others. The mechanism then transforms each token into a weighted average of the feature representations of the other tokens with weights proportional to the learned importance scores. The relative importance scores capture contextual information among tokens and are key to the success of the transformer architecture [72, 67, 5, 51, 31].

Recent work has begun exploring the connections between self-attention and non-parametric kernel regression [46, 19]. Under this interpretation, there is an unknown, underlying function f mapping the tokens in the input sequence to the output sequence. The self-attention mechanism

* Co-first authors.

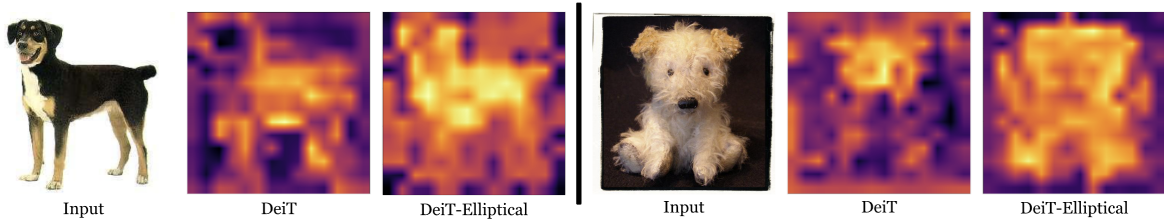


Figure 1: Comparison of Attention Heatmaps. Elliptical pays attention to more relevant information. DeiT focuses on just a subset of informative features while Elliptical considers a wider set of contextually relevant information, helping to produce more accurate and robust predictions. Attention scores are min-max scaled for visualization purposes.

estimates f by performing Nadaraya-Watson (NW) regression with isotropic Gaussian kernels. Our work leverages this perspective on self-attention, where we notice that Gaussian isotropic kernels are spherically invariant. This has the drawback of assuming all dimensions of the feature space are equal in terms of importance, meaning nearby tokens are assigned contextual relevance weights dependant only on their Euclidean distance from a query, regardless of direction. From the non-parametric regression perspective, we show that spherical invariance in the kernel causes the estimator to suffer provably higher variance. This causes two connected disadvantages in the self-attention setting. First, high variance in the estimator impairs robustness as small contaminations in the input cause large, erroneous changes in the self-attention output. Second, the high variance of the estimator reduces the capacity of the self-attention mechanism as hidden representations passing through the model are increasingly composed of uninformative noise.

Contribution. In this work, we propose Elliptical Attention, a new class of self-attention that constructs hyper-ellipsoidal, rather than hyper-spherical, neighborhoods around the attention queries. The key idea is to stretch the neighborhoods around the queries to upweight keys in directions of high importance. We achieve this by computing a Mahalanobis transformation that stretches the axes of the underlying feature space according to a learned measure of coordinate-wise relevance. Constructing hyper-ellipsoidal neighborhoods following this scheme allows the self-attention mechanism to learn higher-quality contextual representations that prevent representation collapse while simultaneously exhibiting stronger robustness. We additionally propose an estimator of coordinate-wise relevance in the self-attention mechanism that can be computed highly efficiently and with no learnable parameters. We theoretically prove that our estimator accurately estimates the relative coordinate-wise relevance in the feature space. Finally, our approach of constructing hyper-ellipsoidal neighborhoods is linked to theoretical improvements in the mean squared error (MSE) of non-parametric estimators by reducing variance without introducing bias. We demonstrate that this provable reduction in variance is related to both representation collapse and robustness, proposing a unifying framework for both phenomena. This framework is based on the geometry of the predictive neighborhood around queries in the attention mechanism. In summary, our contributions are three-fold:

1. We develop the novel Elliptical Attention, which learns better contextual representations by constructing hyper-ellipsoidal neighborhoods around queries.

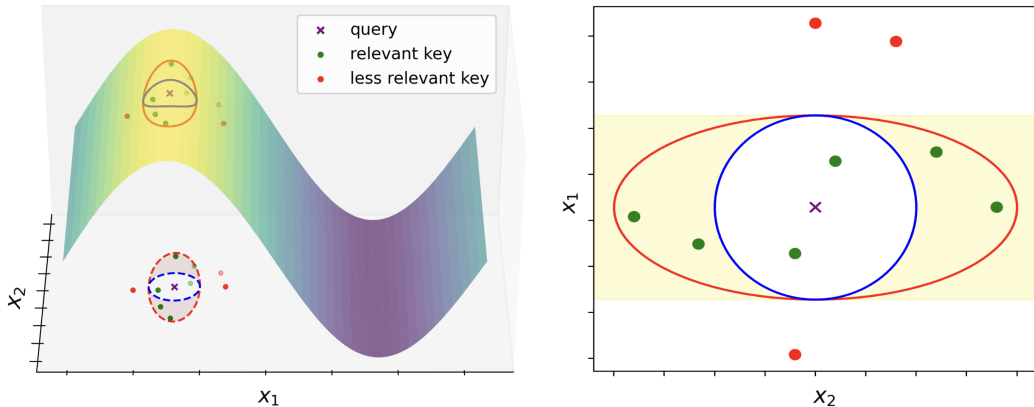


Figure 2: **Left:** The function does not vary in the x_2 axis so we stretch the neighborhood in that direction. **Right:** The stretched ellipsoidal neighborhood includes 4 more keys.

2. We propose an efficient estimator of the coordinate-wise relevance in the self-attention mechanism, which requires no learnable parameters, and provide theoretical guarantees for this estimator.
3. We derive a theoretical framework unifying representation collapse and robustness in transformers based only on the implicit geometry of the attention mechanism.

We empirically demonstrate that 1) Elliptical Attention outperforms baseline self-attention models in terms of accuracy and robustness on a variety of practical benchmarks, including WikiText-103 language modelling, ImageNet-1K object classification, LRA long sequence modeling, and ADE20K image segmentation, 2) Elliptical Attention attains these improvements with lower memory requirements and faster computational speed, and 3) Elliptical Attention can be combined with state-of-the-art robust transformers to further boost robust performance in ImageNet-1K under adversarial attack.

Organization. We structure this paper as follows: In Section 2, we present preliminaries on self-attention and non-parametric kernel regression. In Section 3, we illustrate the theoretical benefits of hyper-ellipsoidal neighborhoods, demonstrate how we build the required transformation, and provide the full technical formulation of Elliptical Attention. We empirically validate the advantages of the Elliptical Attention in Section 4. Related work is discussed in Section 5 before presenting concluding remarks in Section 6. Proofs, technical details, and further experiments are provided in the Appendix.

2 Background: Self-Attention and Non-Parametric Regression

We first provide preliminaries on the self-attention mechanism followed by background on its connection to the Nadaraya-Watson (NW) estimator in non-parametric regression [43].

2.1 Self-Attention Mechanism

Given an input sequence $\mathbf{X} = [\mathbf{x}_1, \dots, \mathbf{x}_N]^\top \in \mathbb{R}^{N \times D_x}$ of N feature vectors, the self-attention mechanism transforms the input to $\mathbf{H} := [\mathbf{h}_1, \dots, \mathbf{h}_N]^\top \in \mathbb{R}^{N \times D_x}$ as follows:

$$\mathbf{h}_i = \sum_{j \in [N]} \text{softmax} \left(\frac{\mathbf{q}_i^\top \mathbf{k}_j}{\sqrt{D}} \right) \mathbf{v}_j, \text{ for } i = 1, \dots, N. \quad (1)$$

The vectors $\mathbf{q}_i, \mathbf{k}_j$, and \mathbf{v}_j are the query, key, and value vectors, respectively. They are computed as $[\mathbf{q}_1, \dots, \mathbf{q}_N]^\top := \mathbf{Q} = \mathbf{X} \mathbf{W}_Q^\top \in \mathbb{R}^{N \times D}$, $[\mathbf{k}_1, \dots, \mathbf{k}_N]^\top := \mathbf{K} = \mathbf{X} \mathbf{W}_K^\top \in \mathbb{R}^{N \times D}$, and $[\mathbf{v}_1, \dots, \mathbf{v}_N]^\top := \mathbf{V} = \mathbf{X} \mathbf{W}_V^\top \in \mathbb{R}^{N \times D_v}$ where $\mathbf{W}_Q, \mathbf{W}_K \in \mathbb{R}^{D \times D_x}$, $\mathbf{W}_V \in \mathbb{R}^{D_v \times D_x}$ are the weight matrices. Eqn. 1 can be expressed in matrix form as:

$$\mathbf{H} = \text{softmax} \left(\frac{\mathbf{Q} \mathbf{K}^\top}{\sqrt{D}} \right) \mathbf{V}, \quad (2)$$

where the softmax function is applied row-wise to the matrix $\mathbf{Q} \mathbf{K}^\top / \sqrt{D}$. Throughout this paper, we refer to transformers built with Eqn. 2 as standard transformers or just transformers.

2.2 A Non-Parametric Regression Perspective of Self-Attention

We now present the connection between self-attention as described in Eqn. 1 and non-parametric regression. We first assume key and value vectors $\{\mathbf{k}_j, \mathbf{v}_j\}_{j \in [N]}$ are obtained from the following data generating process:

$$\mathbf{v} = f(\mathbf{k}) + \boldsymbol{\epsilon}, \quad (3)$$

where $\boldsymbol{\epsilon}$ is random zero-mean noise $\mathbb{E}[\boldsymbol{\epsilon}] = 0$, and f is the unknown function to be estimated. We consider the random design setting where the keys $\{\mathbf{k}_j\}_{j \in [N]}$ are i.i.d samples drawn from the marginal distribution $p(\mathbf{k})$. We use $p(\mathbf{v}, \mathbf{k})$ to denote the joint distribution of pairs (\mathbf{v}, \mathbf{k}) as obtained according to Eqn. 3. At any given new query \mathbf{q} , we aim to estimate the unknown function $f(\mathbf{q})$.

The NW estimator is a non-parametric estimator of the unknown f described by

$$f(\mathbf{k}) = \mathbb{E}[\mathbf{v} | \mathbf{k}] = \int_{\mathbb{R}^D} \mathbf{v} \cdot p(\mathbf{v} | \mathbf{k}) d\mathbf{v} = \int_{\mathbb{R}^D} \frac{\mathbf{v} \cdot p(\mathbf{v}, \mathbf{k})}{p(\mathbf{k})} d\mathbf{v}, \quad (4)$$

where we apply zero-mean noise for the first equality and the definitions of conditional expectation and density for the second and final. Then, it can be shown that by estimating the joint density $p(\mathbf{v}, \mathbf{k})$ and marginal density $p(\mathbf{k})$ using isotropic Gaussian kernels with bandwidth σ and evaluating the NW estimator at a new query \mathbf{q}_i , we obtain

$$\hat{f}_\sigma(\mathbf{q}_i) = \frac{\sum_j^N \mathbf{v}_j \exp(-\|\mathbf{q}_i - \mathbf{k}_j\|^2 / 2\sigma^2)}{\sum_j^N \exp(-\|\mathbf{q}_i - \mathbf{k}_j\|^2 / 2\sigma^2)} \quad (5)$$

$$= \frac{\sum_j^N \mathbf{v}_j \exp(\mathbf{q}_i^\top \mathbf{k}_j / \sigma^2)}{\sum_j^N \exp(\mathbf{q}_i^\top \mathbf{k}_j / \sigma^2)} = \sum_{j \in [N]} \text{softmax}(\mathbf{q}_i^\top \mathbf{k}_j / \sigma^2) \mathbf{v}_j, \quad (6)$$

where choosing $\sigma^2 = \sqrt{D}$ as the isotropic variance recovers the full attention mechanism. We present the full derivation in Appendix A.

Limitation of self-attention. We see in Eqn. 5 that standard self-attention computes the relative importance scores between queries and keys via Euclidean distance. Euclidean distances are spherically invariant and therefore fail to consider coordinate-wise significance in the feature space, meaning the proximity of \mathbf{k}_j from \mathbf{q}_i influences its contextual relevance equally regardless of direction.

3 Elliptical Attention: Leveraging Hyper-Ellipsoids to Pay More Attention Without Losing Focus

In this section, we begin by presenting how NW regression obtains a lower MSE by taking hyper-ellipsoidal neighborhoods around queries. We then construct the required hyper-ellipsoidal transformation via a Mahalanobis distance metric. We present the framework relating robustness and representation collapse to the geometry of the query neighborhoods and show how our proposed scheme offers improvements in both areas. We then provide an efficient estimator of the coordinate-wise relevance before finally giving the full technical formulation of Elliptical Attention. We provide technical details on the implementation procedure in Appendix E.

3.1 Improving NW Regression with Hyper-Ellipsoids

Distance-based estimators, such as the NW estimator, can obtain a lower MSE by taking hyper-ellipsoidal neighborhoods around queries [24, 25]. The key idea is that we wish to stretch the axes of the underlying space in directions for which the true f in Eqn. 3 varies least.

Figure 2 shows a situation in which f does not vary equally in all directions. This is actually a limiting case in which the function is sparse in the x_2 direction. If we stretched the Euclidean circular neighborhoods around each query into the shown ellipse, we include more data in the x_2 direction which helps obtain a lower variance estimator. Intuitively, this follows from the well-established result in non-parametric estimation that the variance of an estimate at a point is inversely proportional to the number of samples in that point’s neighborhood [18]. Crucially, this does not introduce bias into the estimate because the function does not vary in the x_2 direction, and so including these additional samples does not smooth out the true variation.

This intuition is formalized in Theorem 1 in Appendix C, which shows that the best achievable rate of convergence for estimators of non-sparse Lipschitz functions is of the order $\mathcal{O}(n^{-2/(2+d)})$ for a d dimensional feature space. However, when the function only depends on $R \subseteq [d]$ coordinates, the rate improves to $\mathcal{O}(n^{-2/(2+|R|)})$. In the case of approximate sparsity, when coordinate directions exhibit differing variability, the same intuition carries over as shown by the improvement in convergence rates in Theorem 2 in Appendix C.

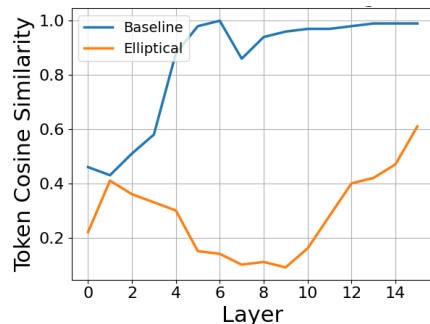


Figure 3: Representation Collapse on WikiText-103. Elliptical Attention learns more diverse representations.

We leverage this analysis from non-parametric regression to motivate our Elliptical Attention. From the regression perspective, the self-attention mechanism, which performs NW regression, is able to learn a lower MSE estimator of the true underlying f by reducing the variance of the estimator without (or with minimal) introduction of bias. From the attention perspective, this means queries pay higher attention to more relevant keys, producing more contextually meaningful attention scores and better, more robust learned representations.

3.2 Capturing Coordinate-wise Variability and Building the Mahalanobis Transformation

We measure the variation in f in the i^{th} coordinate direction by the expectation of the \mathcal{L}_1 norm of the i^{th} directional derivative taken over all $k \in \mathcal{X}_k$, where $\mathcal{X}_k \subseteq \mathbb{R}^D$ denotes the feature space. Roughly speaking, this quantity corresponds to the average absolute gradient of f in the i^{th} direction throughout the space. Formally, this quantity is defined as

Definition 1 (Coordinate-wise Variability of $f : \mathbb{R}^D \rightarrow \mathbb{R}^{D_v}$) *The coordinate-wise variability of $f : \mathbb{R}^D \rightarrow \mathbb{R}^{D_v}$ with Jacobian matrix $\mathbf{J}_f \in \mathbb{R}^{D_v \times D}$ in the i^{th} direction is given by the quantity $\|f'_i\|_{1,\mu} := \mathbb{E}_{\mathbf{k} \sim \mu} \|\mathbf{J}_f(\mathbf{k})\mathbf{e}_i\|_1, i \in [D]$, where \mathbf{e}_i is an all-zero vector with a single 1 in the i^{th} coordinate and μ is the marginal distribution of k over support \mathcal{X}_k .*

Remark 1 *This definition is one of many possible. One could also take the supremum rather than the expectation or consider second derivatives. We select this definition as averages over first derivatives are more easily estimated and the definition still captures the intuitive properties of variability.*

Denoting estimates of the coordinate-wise variability $\|f'_i\|_{1,\mu}$ by m_i , we can then incorporate these quantities into a distance function of the form

$$d(\mathbf{q}, \mathbf{k}) := \sqrt{(\mathbf{q} - \mathbf{k})^\top \mathbf{M}(\mathbf{q} - \mathbf{k})}, \quad (7)$$

where $\mathbf{M} = \text{diag}(m_1, m_2, \dots, m_D)$ is a diagonal matrix whose diagonal elements are the estimates of $\|f'_i\|_{1,\mu}$ for $i \in [D]$.

Remark 2 *The metric described in Eqn. 7 takes the form of a Mahalanobis distance metric, which can be interpreted as first applying a transformation to the underlying space in which we stretch the coordinate axes by the diagonal elements of \mathbf{M} . Therefore using this metric within the self-attention computation produces the desired hyper-ellipsoidal neighborhoods around queries.*

Remark 3 *In practice, we maxscale the estimates to obtain $m_i \leftarrow m_i/m_{\max}$ where $m_{\max} \geq m_i$ for all $i \in [D]$. This is because we care about the relative magnitudes of the direction-wise variability as opposed to the absolute magnitudes. Under this interpretation, we identify the most variable dimension and stretch all others relative to this direction.*

3.3 Promoting Robustness and Avoiding Representation Collapse

We illustrate how robustness and representation collapse connect to the hyper-ellipsoidal transformation and the variance of the self-attention estimator. We show how Elliptical Attention offers improvements in both areas.

Dimension-wise input sensitivity of Elliptical Attention and robustness. In Lemma 1, we show that when each input component is weighted differently, which corresponds to using the Mahalanobis transformation as in Eqn. 7, the impact of perturbing the i^{th} input coordinate on any coordinate of the transformed softmax output, defined as in Eqn. 8, becomes proportional to the corresponding weighting parameter with proportionality coefficient depending on the indices i and j .

Lemma 1 *Let $\mathcal{M} : \mathbb{R}^D \rightarrow \mathbb{R}^N$ denote the transformed Elliptical softmax operator for a given set of keys as*

$$\mathcal{M}(\mathbf{x}) := \frac{1}{\sum_{j \in [N]} \exp(\mathbf{xMk}_j)} \begin{bmatrix} \exp(\mathbf{xMk}_1) \\ \exp(\mathbf{xMk}_2) \\ \vdots \\ \exp(\mathbf{xMk}_N) \end{bmatrix}, \quad (8)$$

for weight matrix \mathbf{M} as in Eqn. 7. Then, the achievable rate of change of $\mathcal{M}(\mathbf{x})$ in i^{th} input dimension is proportional to m_i , that is, for all $i \in [D]$ and $j \in [N]$,

$$\sup_{\mathbf{x} \in \mathcal{X}} |\mathbf{J}_{\mathcal{M}}(\mathbf{x})_{ji}| \propto m_i, \quad (9)$$

where $\mathbf{J}_{\mathcal{M}}$ is the Jacobian matrix of \mathcal{M} .

By virtue of Lemma 1, which is proven in Appendix B.1, we show in Proposition 1 that choosing the weights as properly scaled estimates of the underlying function variability, as in Elliptical Attention, the output vectors become less prone to large errors caused by noisy input while simultaneously respecting the dimension-wise variability pattern of the true self-attention function.

Proposition 1 (Robustness of Elliptical Attention) *Let $f : \mathbb{R}^D \rightarrow \mathbb{R}^{D_v}$ be the true self-attention function, \hat{f}_d be the Elliptical Attention estimator with metric d as described in Eqn. 7. Then for any index $i \in [N]$ and noise $\epsilon \in \mathbb{R}^D$, the following error bound holds*

$$\|\hat{f}_d(\mathbf{q}_i) - \hat{f}_d(\mathbf{q}_i + \epsilon)\| \leq \left(\sum_{j \in [N]} \sqrt{\text{tr}(\mathbf{K}_j^2 \mathbf{M}^2)} \|\mathbf{v}_j\| \right) \|\epsilon\|, \quad (10)$$

where $\{\mathbf{K}_j\}_{j \in [N]}$ are constant diagonal matrices that depend only on the key vectors.

Note that when the estimates are maxscaled so that $m_i \leq 1$, the achievable output error of Elliptical Attention is lower than that of standard self-attention where $m_i = 1$ for all $i \in [D]$. Besides, when the true function exhibits approximate sparsity in some number of dimensions

(i.e. $m_i \rightarrow 0^+$ for majority of indices), the error bound in 10 becomes significantly tighter for Elliptical Attention. The proof of Proposition 1 is provided in Appendix B.2.

Input smoothing and representation collapse. In each layer, the standard self-attention mechanism fits a noisy estimate of the true function f , which is then fed into subsequent layers and iteratively refit. The input to each attention layer is then partially composed of noise, which is equivalently the common regularization method of random input smoothing. We show that by reducing the noise component in each layer, Elliptical Attention maintains expressive power and resists representation collapse. This is formalized in the following proposition:

Proposition 2 (Elliptical Attention maintains expressive power by reducing noise) *Let \mathbf{h}_d^ℓ denote the output of a transformer using Elliptical Attention with metric d as described in Eqn. 7 and \mathbf{h}^ℓ denote the output of a transformer using standard self-attention at layer ℓ . Let \mathcal{D} be the sampling distribution of the data and let $\mathbf{c} \in \mathbb{R}^D$. Then, for any \mathbf{h}, \mathbf{h}_d and layer ℓ , in expectation a standard self-attention transformer attenuates towards \mathbf{c} faster than Elliptical Attention. Formally, we have:*

$$\mathbb{E}_{\mathcal{D}} \|\mathbf{h}_d^\ell - \mathbf{c}\| \geq \mathbb{E}_{\mathcal{D}} \|\mathbf{h}^\ell - \mathbf{c}\|. \quad (11)$$

Proof is provided in Appendix B.3. Proposition 2 shows that Elliptical Attention maintains better expressive power over standard self-attention. We find this to be empirically substantiated as shown in Figure 3.

3.4 An Efficient Estimator of the Coordinate-wise Variability

We propose a simple difference-based estimator that effectively captures the coordinate-wise variability of the underlying function. Our estimator is easily and efficiently computed. It requires no additional learnable parameters and demands negligible additional memory. Let \mathbb{E}_n denote empirical mean over n samples, $\mathbf{v}^\ell(i)$ denote the i^{th} component of the vector \mathbf{v} at the ℓ^{th} layer, and $\mathcal{X}_v^{\ell, \ell+1} = \{(\mathbf{v}^{\ell+1}, \mathbf{v}^\ell) : \mathbf{v}^\ell = f(\mathbf{k}^\ell) + \epsilon\}$ be the value feature space at neighboring layers ℓ and $\ell + 1$ where values are generated according to the process described in Eqn. 3. Then, our approach to estimating the i^{th} coordinate-wise variability is described in the following proposition.

Proposition 3 (Coordinate-wise Variability Estimator) *Given a function $f : \mathbb{R}^D \rightarrow \mathbb{R}^{D_v}$ with i^{th} directional variation $\|f'_i\|_{1, \mu}, i \in [D]$ and some $\delta > 0$, the directional variation can be estimated by the quantity*

$$m_i := \mathbb{E}_n \frac{|\mathbf{v}^{\ell+1}(i) - \mathbf{v}^\ell(i)|}{\delta} \Big|_{(\mathbf{v}^\ell, \mathbf{v}^{\ell+1}) \in \mathcal{X}_v^{\ell, \ell+1}}. \quad (12)$$

Remark 4 *For the purposes of improving the performance of transformers by stretching the feature space according to the direction-wise variability of f , we note that consistent estimators of $\|f'_i\|_{1, \mu}$ for all $i \in [D]$ are sufficient but not necessary. Instead, we require only the weaker objective of accurately estimating the relative magnitudes of the direction-wise variability. That is, if $\|f'_i\|_{1, \mu} \geq \|f'_j\|_{1, \mu}$, we need only that $m_i \geq m_j$. This is because the theory requires us only to identify coordinate directions of more or less variability and shrink or stretch the space accordingly.*

The intuition behind our estimator in Eqn. 12 lies in prior lines of research dedicated to studying transformers as an Euler discretization of some continuous-time dynamics, usually as a system of first-order ODEs [35, 16, 47]. In fact, our estimator resembles the absolute value of a forward Euler discretization of the variability of the i^{th} component of a value vector over time $\partial \mathbf{v}(i, t)/\partial t$, where the layers ℓ and $\ell + 1$ represent consecutive time points in a time interval partition with the step size δ . We prove that our estimator in Eqn. 12 effectively estimates the relative magnitudes of the coordinate-wise variability of f in Appendix B.4.

3.5 Full Technical Formulation of Elliptical Attention

We now present the full formulation of Elliptical Attention.

Definition 2 (Elliptical Attention Computation) *Let φ_σ denote the Gaussian isotropic density kernel with variance $\sigma^2 \mathbf{I}$ and $d(\cdot, \cdot)$ be the metric as defined in Eqn. 7, then the Elliptical Attention output $\hat{\mathbf{h}}_i$ for the i th query \mathbf{q}_i given keys $\{\mathbf{k}_j\}_{j=1}^N$ and values $\{\mathbf{v}_j\}_{j=1}^N$ is given by*

$$\begin{aligned} \hat{\mathbf{h}}_i &:= \hat{f}_{d,D}(\mathbf{q}_i) = \sum_{j \in [N]} \frac{\varphi_\sigma(d(\mathbf{q}_i, \mathbf{k}_j)/\sigma^2) \mathbf{v}_j}{\sum_{j \in [N]} \varphi_\sigma(d(\mathbf{q}_i, \mathbf{k}_j)/\sigma^2)} \\ &= \sum_{j \in [N]} \frac{\exp(\mathbf{q}_i^\top \mathbf{M} \mathbf{k}_j / \sqrt{D}) \mathbf{v}_j}{\sum_{j \in [N]} \exp(\mathbf{q}_i^\top \mathbf{M} \mathbf{k}_j / \sqrt{D})} = \sum_{j \in [N]} \text{softmax}(\mathbf{q}_i^\top \mathbf{M} \mathbf{k}_j / \sigma^2) \mathbf{v}_j, \end{aligned} \quad (13)$$

where $\sigma^2 = \sqrt{D}$. Eqn. 13 is equivalently expressed in matrix form as

$$\mathbf{H} = \text{softmax} \left(\frac{\mathbf{Q} \mathbf{M} \mathbf{K}^\top}{\sqrt{D}} \right) \mathbf{V}. \quad (14)$$

Remark 5 *We see from the form of Eqn. 13 that standard self-attention is recoverable by setting $\mathbf{M} = \mathbf{I}_D$. Under our framework, this implies that standard self-attention assumes the underlying regression function to have exactly equal variability in all coordinate directions.*

4 Experimental Results

In this section, we numerically justify the advantage of Elliptical Attention over baseline transformers that take hyper-spheres around queries. We evaluate our method on robust Wikitext-103 modelling under Word Swap contamination [40], ImageNet classification under a wide range of attacks [11, 58], the Long Range Arena benchmark [65], and ADE20K image segmentation [76]. We aim to show that i) Elliptical Attention offers substantive improvements over baseline models across tasks on both clean and contaminated data; ii) Elliptical Attention attains these improvements while reducing memory requirements and increasing computational speed; iii) Elliptical Attention can be combined with state-of-the-art robust transformers to further improve robustness without any increase in computational overhead.

We compare Elliptical Attention with baselines of the same configuration. Results are averaged over 5 runs with different seeds. Additional results and details on experimental procedure are provided in Appendix F.

Table 1: Perplexity (PPL) on WikiText-103 under Word Swap contamination. Elliptical achieves top PPL in clean data and second best in contaminated. Best result in bold and second best underlined.

Model	Clean Test PPL (\downarrow)	Contaminated Test PPL (\downarrow)
<i>Transformer</i> [71]	34.29	74.56
Performer [6]	33.49	73.48
Transformer-MGK [48]	33.21	71.03
FourierFormer [46]	32.85	68.33
Transformer-SPKDE [19]	<u>32.18</u>	54.97
Transformer-MoM [19]	34.68	52.14
Transformer-Elliptical	32.00	<u>52.59</u>

Table 2: Top-1 and Top-5 Test accuracy on ImageNet under adversarial attacks PGD, FGSM, and SPSA with perturbation budget 1/255. Best result shown in bold and second best shown underlined.

Method	Clean Data		FGSM		PGD		SPSA	
	Top 1	Top 5	Top 1	Top 5	Top 1	Top 5	Top 1	Top 5
<i>DeiT</i> [68]	72.23	91.13	52.61	82.26	41.84	76.49	48.34	79.36
Distill [68]	<u>74.32</u>	<u>93.72</u>	53.24	84.07	41.72	76.43	49.56	80.14
FourierFormer [46]	73.25	91.66	53.08	83.95	41.34	76.19	48.79	79.57
RVT [39]	74.37	93.89	53.67	84.11	43.39	77.26	<u>51.43</u>	<u>80.98</u>
DeiT-KDE [19]	72.58	91.34	52.25	81.52	41.38	76.41	48.61	79.68
DeiT-MoM [19]	71.94	91.08	55.76	85.23	<u>43.78</u>	<u>78.85</u>	49.38	80.02
DeiT-Elliptical	72.36	91.33	<u>54.64</u>	<u>85.18</u>	44.96	79.35	56.55	87.26

Robust Language Modelling. Table 1 shows our Elliptical Transformer (*Elliptical*) achieves top test perplexity in clean data while also achieving second top test perplexity under data contamination by Word Swap [42], illustrating Elliptical Attention is both highly robust and offers substantial advantages on clean data as well.

Image Classification under Adversarial Attack. Table 2 shows the results of white box attacks FGSM [17] and PGD [37], and black box attack SPSA [70]. *Elliptical* attains top robustness in PGD and SPSA and second top in FGSM while achieving highly competitive clean accuracy. *DeiT-Elliptical* is particularly impressive under black box attack SPSA, improving over the next best model, Robust Vision Transformer (*RVT*) [39], by 10%.

Table 4 shows results on Auto Attack [8], which is an ensemble of white and black box attacks APGD-CE, APGD-T, FAB-T, and Square. We display results for attacks individually as well as when applied in default sequential mode. *DeiT-Elliptical* substantially outperforms standard *DeiT* in each attack individually and sequentially. We again notice strong performance against black box attack Square with an 8.5% improvement. When combining with state-of-the-art

Table 3: Top-1 Test accuracy on LRA tasks equation calculation (ListOps), review classification (Text), document retrieval (Retrieval), image classification (Image) and spatial dependencies (Pathfinder). Best result in bold and second best underlined.

Dataset (seq. length)	<i>Trans.</i> [71]	<i>Lin.</i> [21]	<i>Re.</i> [23]	<i>Per.</i> [6]	<i>Long.</i> [3]	<i>Elliptical</i>
ListOps (2K)	37.1	<u>37.3</u>	19.1	18.8	37.2	37.8
Text (4K)	<u>65.0</u>	55.9	64.9	63.8	64.6	65.6
Retrieval (4K)	79.4	79.4	78.6	78.6	81.0	<u>80.3</u>
Image (1K)	38.2	37.8	43.3	37.1	39.1	<u>40.2</u>
Pathfinder (1K)	74.2	67.6	69.4	69.9	73.0	<u>73.2</u>
Average Accuracy	58.5	55.6	55.1	53.6	<u>59.0</u>	59.4

Table 4: Top-1 and Top-5 Test accuracy on ImageNet under Auto Attack with perturbation budget 1/255. Results are displayed both for the default sequential attack, where attacks are applied successively, and also for each attack individually. Best result is shown in bold.

Method	<i>DeiT</i> [68]		DeiT-Elliptical		<i>FAN</i> [56]		FAN-Elliptical	
	Top 1	Top 5	Top 1	Top 5	Top 1	Top 5	Top 1	Top 5
Clean Data	72.23	91.13	72.36	91.33	76.31	93.42	76.38	93.53
APGD-CE	27.75	66.48	31.27	68.28	35.05	74.56	36.13	75.69
APGD-T	27.74	73.37	29.69	74.39	35.02	80.46	36.25	81.30
FAB-T	71.61	90.54	71.74	90.81	76.35	93.65	76.16	93.45
Square	43.55	80.96	47.25	81.65	56.75	88.05	58.38	88.20
Average	42.66	77.84	45.00	78.78	50.79	84.18	51.73	84.66
Sequential Attack	26.08	64.18	27.45	67.77	33.29	74.52	34.54	75.67

robust transformer *FAN* [35], Elliptical Attention improves robustness to sequential Auto Attack and all individual attacks except FAB-T, for which it still remains highly competitive. This shows Elliptical Attention can further boost robustness when combined with state-of-the-art robust models.

Long Sequence Modelling on the LRA Benchmark. Table 3 shows the results of Elliptical Attention assessed on the LRA long sequence benchmark. Elliptical Attention achieves top or second top test accuracy in every task and top overall performance. This shows Elliptical Attention learns superior representations across a wide range of modalities in long-range contexts.

Image Segmentation on ADE20K. Table 5 reports pixel accuracy, mean accuracy, and mean intersection over union (IOU) on the ADE20K segmentation task. Elliptical Attention boosts performance across all metrics, with intersection over union, in particular, improving by a substantive 4.7%. This result shows Elliptical Attention is able to improve performance across a variety of modalities.

Table 5: Image Segmentation Results

Model	Pixel Acc.	Avg Acc.	Avg IOU
<i>DeiT</i> [68]	77.93	46.30	35.44
<i>Elliptical</i>	78.46	48.04	37.09

Table 6: Wikitext-103 Results

Model	Test PPL (\downarrow)
<i>Transformer-small</i> [71]	34.29
<i>Elliptical-small</i>	32.00
<i>Transformer-medium</i> [71]	29.60
<i>Elliptical-medium</i>	27.60

Further Clean Data Language Modelling. We present in Table 6 additional results on clean Wikitext-103 when evaluating Elliptical Attention on a larger model configuration to show Elliptical’s ability to scale with model size. We observe that with a medium-sized transformer backbone, Elliptical Attention maintains a similarly substantial improvement over the baseline.

5 Related Work

Theoretical Frameworks for Attention. Attention mechanisms have been studied from a range of perspectives. [69] show that attention can be derived from kernel similarity functions and [64] explain attention through nonlinear singular value decomposition of asymmetric kernels. Attention has also been explained through ordinary/partial differential equations, Gaussian mixture models, and graph-structured learning [35, 59, 63, 15, 48, 26, 75]. [46, 19] show that self-attention performs Nadaraya-Watson regression with Gaussian isotropic kernels. This paper leverages this viewpoint and proposes modifying the Gaussian isotropic kernels to include a Mahalanobis metric which can be interpreted as stretching the hyper-spherical neighborhoods of the kernel to hyper-ellipsoids.

Robust Transformers. Existing work in robust transformers tends to propose modality-specific approaches. In vision, [38] propose an ensemble defense strategy to white-box attacks while [39] propose position-aware attention scaling and patch-wise augmentation. Recently, [78] propose the fully-attentional network to attain state-of-the-art accuracy on corrupted image data. In language, [74] propose structurally aware table-text encoding, [33] propose a robust end-to-end transformer for crisis detection, and [28] propose duration-based hard attention. These methodologies are typically motivated by their respective domain and tend to have limited generalizability to differing domains. Our approach, by contrast, proposes a general framework that makes no assumption on the downstream task and requires no additional parameters and negligible computational overhead.

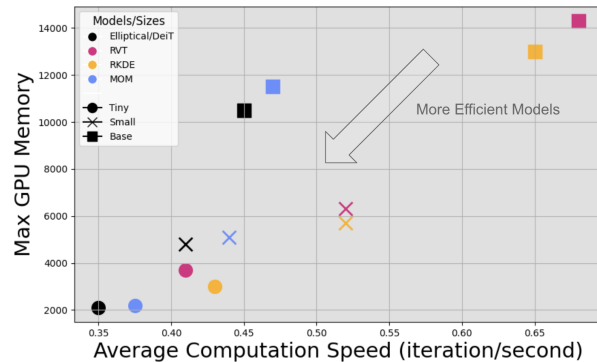


Figure 4: ImageNet Efficiency: Deit, Elliptical, RVT, RKDE, MOM on Tiny, Small, and Base sizes. Elliptical is the most efficient robust model. DeiT and Elliptical are shown as the same data point as their efficiency is indistinguishable.

Mahalanobis Metrics. Mahalanobis metrics have been used predominantly in classical machine learning algorithms. In nearest-neighbor (NN) classification and regression, [73, 44] learn the metric through backpropagation. In NN KL divergence estimation, [50] learn a Mahalanobis metric from density approximation. In kernel regression, [49] take eigenvalues of the estimated Jacobian while [24, 25] estimate coordinate-wise variability of the true function. Our model similarly uses coordinate-wise variability of the unknown function to form the Mahalanobis transformation but instead uses a more efficient estimator that does not require materializing the prediction function and accommodates the self-attention setting. In general, our method is among the early work in incorporating Mahalanobis metrics into the self-attention mechanism.

6 Conclusion and Future Work

In this paper, we present Elliptical Attention, a novel variant of attention that computes a Mahalanobis transformation to stretch the underlying feature space in directions of high contextual relevance. This transformation can be interpreted as modifying the hyper-spherical neighborhoods around queries to hyper-ellipsoids which upweight the attention paid to keys lying in important directions, enabling the transformer to learn better and more robust representations. This approach makes no assumptions on the downstream task, requires no learnable parameters, and can be applied to any transformer to boost clean and robust performance. A limitation of our work is that we use the values over layers to estimate the average direction-wise gradient of the true self-attention function, which makes the estimate prone to noise. For ongoing work, we are exploring more precise estimation methods with provable convergence guarantees that do not compromise efficiency.

Supplement to “Elliptical Attention”

Table of Contents

A	Full Derivation of Self-Attention as Non-Parametric Regression	14
B	Technical Proofs	15
B.1	Proof of Lemma 1	15
B.2	Proof of Proposition 1	17
B.3	Proof of Proposition 2	17
B.4	Proof of Proposition 3	19
B.5	Lipschitz smoothness in (\mathcal{X}, d)	22
C	Additional Theorems	23
D	A Consistent Estimator	24
E	Implementation Procedure and Computational Efficiency	25
F	Experimental Details and Additional Experiments	26
F.1	Out-of-Distribution Robustness and Data Corruption on ImageNet-A,R,C . . .	26
F.2	Representation Collapse	26
F.3	Head Redundancy	27
F.4	Wikitext-103 Language Modelling and Word Swap Attack	27
F.5	ImageNet Image Classification and Adversarial Attack	28
F.6	LRA Long Sequence Classification.	29
F.7	ADE20K Image Segmentation	29
F.8	Ablation Studies	30
G	Broader Impacts	31

A Full Derivation of Self-Attention as Non-Parametric Regression

Recall NW estimator is a non-parametric estimator of the unknown f at any given query \mathbf{q} described by

$$f(\mathbf{k}) = \mathbb{E}[\mathbf{v}|\mathbf{k}] = \int_{\mathbb{R}^D} \mathbf{v} \cdot p(\mathbf{v}|\mathbf{k})d\mathbf{v} = \int_{\mathbb{R}^D} \frac{\mathbf{v} \cdot p(\mathbf{v}, \mathbf{k})}{p(\mathbf{k})}d\mathbf{v},$$

where the first equality comes from the noise being zero mean, the second equality comes from the definition of conditional expectation and the final equality comes from the definition of conditional density. Eqn. 3 implies that if we can just obtain good estimates of the joint density $p(\mathbf{v}, \mathbf{k})$ and marginal density $p(\mathbf{k})$ then we can estimate the required $f(\mathbf{q})$. The Gaussian isotropic kernels with bandwidth σ are given by

$$\hat{p}_\sigma(\mathbf{v}, \mathbf{k}) = \frac{1}{N} \sum_{j \in [N]} \varphi_\sigma(\mathbf{v} - \mathbf{v}_j)\varphi_\sigma(\mathbf{k} - \mathbf{k}_j), \quad \hat{p}_\sigma(\mathbf{k}) = \frac{1}{N} \sum_{j \in [N]} \varphi_\sigma(\mathbf{k} - \mathbf{k}_j), \quad (15)$$

where φ_σ is the multivariate Gaussian density function with diagonal covariance matrix $\sigma^2 \mathbf{I}_D$. Given the kernel density estimators in Eqn. 15, the unknown function can be estimated as

$$\begin{aligned}\hat{f}_\sigma(\mathbf{k}) &= \int_{\mathbb{R}^D} \frac{\mathbf{v} \cdot \hat{p}_\sigma(\mathbf{v}, \mathbf{k})}{\hat{p}_\sigma(\mathbf{k})} d\mathbf{v} = \int_{\mathbb{R}^D} \frac{\mathbf{v} \cdot \sum_{j \in [N]} \varphi_\sigma(\mathbf{v} - \mathbf{v}_j) \varphi_\sigma(\mathbf{k} - \mathbf{k}_j)}{\sum_{j \in [N]} \varphi_\sigma(\mathbf{k} - \mathbf{k}_j)} d\mathbf{v} \\ &= \frac{\sum_{j \in [N]} \varphi_\sigma(\mathbf{k} - \mathbf{k}_j) \int \mathbf{v} \cdot \varphi_\sigma(\mathbf{v} - \mathbf{v}_j) d\mathbf{v}}{\sum_{j \in [N]} \varphi_\sigma(\mathbf{k} - \mathbf{k}_j)} = \frac{\sum_{j \in [N]} \mathbf{v}_j \varphi_\sigma(\mathbf{k} - \mathbf{k}_j)}{\sum_{j \in [N]} \varphi_\sigma(\mathbf{k} - \mathbf{k}_j)}.\end{aligned}$$

Then, using the definition of the Gaussian isotropic kernel and evaluating the estimated function at \mathbf{q}_i we have

$$\begin{aligned}\hat{f}(\mathbf{q}_i) &= \frac{\sum_j^N \mathbf{v}_j \exp(-\|\mathbf{q}_i - \mathbf{k}_j\|^2/2\sigma^2)}{\sum_j^N \exp(-\|\mathbf{q}_i - \mathbf{k}_j\|^2/2\sigma^2)} \\ &= \frac{\sum_j^N \mathbf{v}_j \exp[-(\|\mathbf{q}_i\|^2 + \|\mathbf{k}_j\|^2)/2\sigma^2] \exp(\mathbf{q}_i^\top \mathbf{k}_j/\sigma^2)}{\sum_j^N \exp[-(\|\mathbf{q}_i\|^2 + \|\mathbf{k}_j\|^2)/2\sigma^2] \exp(\mathbf{q}_i^\top \mathbf{k}_j/\sigma^2)} \\ &= \frac{\sum_j^N \mathbf{v}_j \exp(\mathbf{q}_i^\top \mathbf{k}_j/\sigma^2)}{\sum_j^N \exp(\mathbf{q}_i^\top \mathbf{k}_j/\sigma^2)} = \sum_{j \in [N]} \text{softmax}(\mathbf{q}_i^\top \mathbf{k}_j/\sigma^2) \mathbf{v}_j.\end{aligned}$$

B Technical Proofs

In this section, we present the omitted theorem statements and technical proofs in the main body of the paper.

B.1 Proof of Lemma 1

Let $\mathcal{M} : \mathbb{R}^D \rightarrow \mathbb{R}^N$ be the transformed softmax operator as defined in the proposition. We wish to find its Jacobian matrix given by

$$\mathbf{J}_{\mathcal{M}}(\mathbf{q}) = \begin{bmatrix} \frac{\partial \mathcal{M}_1(\mathbf{q})}{\partial q^1} & \frac{\partial \mathcal{M}_1(\mathbf{q})}{\partial q^2} & \cdots & \frac{\partial \mathcal{M}_1(\mathbf{q})}{\partial q^D} \\ \frac{\partial \mathcal{M}_2(\mathbf{q})}{\partial q^1} & \frac{\partial \mathcal{M}_2(\mathbf{q})}{\partial q^2} & \cdots & \frac{\partial \mathcal{M}_2(\mathbf{q})}{\partial q^D} \\ \vdots & \vdots & \ddots & \vdots \\ \frac{\partial \mathcal{M}_N(\mathbf{q})}{\partial q^1} & \frac{\partial \mathcal{M}_N(\mathbf{q})}{\partial q^2} & \cdots & \frac{\partial \mathcal{M}_N(\mathbf{q})}{\partial q^D} \end{bmatrix},$$

to measure the sensitivity of each output dimension to a change in each input dimension. Let $\mathcal{M}_j : \mathbb{R}^D \rightarrow \mathbb{R}$ denote the j^{th} component of the output vector for $j \in [N]$, that is, for a vector $\mathbf{q} \in \mathbb{R}^D$,

$$\mathcal{M}_j(\mathbf{q}) = \frac{\exp(\mathbf{q}^\top \mathbf{M} \mathbf{k}_j)}{\sum_{s \in [N]} \exp(\mathbf{q}^\top \mathbf{M} \mathbf{k}_s)}. \quad (17)$$

Let q^i and k_j^i denote the i^{th} coordinates of vectors \mathbf{q} and \mathbf{k}_j , respectively. Then,

$$\begin{aligned}
\frac{\partial}{\partial q^i} \ln(\mathcal{M}_j(\mathbf{q})) &= \frac{\partial}{\partial q^i} \left(\mathbf{q}^\top \mathbf{M} \mathbf{k}_j - \ln \left(\sum_{s \in [N]} \exp(\mathbf{q}^\top \mathbf{M} \mathbf{k}_s) \right) \right) \\
&= m_i k_j^i - \frac{\sum_{s \in [N]} \frac{\partial}{\partial q^i} \exp(\mathbf{q}^\top \mathbf{M} \mathbf{k}_s)}{\sum_{s \in [N]} \exp(\mathbf{q}^\top \mathbf{M} \mathbf{k}_s)} \\
&= m_i k_j^i - m_i \sum_{s \in [N]} \frac{k_s^i \exp(\mathbf{q}^\top \mathbf{M} \mathbf{k}_s)}{\sum_{s' \in [N]} \exp(\mathbf{q}^\top \mathbf{M} \mathbf{k}_{s'})} \\
&= m_i \left(k_j^i - \sum_{s \in [N]} k_s^i \mathcal{M}_s(\mathbf{q}) \right).
\end{aligned}$$

Since the output of Eqn. 8 consists of only positive components, we have

$$\begin{aligned}
\frac{\partial}{\partial q^i} \mathcal{M}_j(\mathbf{q}) &= \frac{\partial}{\partial q^i} \ln(\mathcal{M}_j(\mathbf{q})) \cdot \mathcal{M}_j(\mathbf{q}) \\
&= m_i \left(k_j^i - \sum_{s \in [N]} k_s^i \mathcal{M}_s(\mathbf{q}) \right) \mathcal{M}_j(\mathbf{q}).
\end{aligned}$$

Therefore, the triangle inequality gives

$$\begin{aligned}
\left| \frac{\partial}{\partial q^i} \mathcal{M}_j(\mathbf{q}) \right| &= \left| m_i \left(k_j^i - \sum_{s \in [N]} k_s^i \mathcal{M}_s(\mathbf{q}) \right) \mathcal{M}_j(\mathbf{q}) \right| \\
&\leq m_i \left(|k_j^i (1 - \mathcal{M}_j(\mathbf{q})) \mathcal{M}_j(\mathbf{q})| + \sum_{s \in [N] \setminus \{j\}} |k_s^i \mathcal{M}_s(\mathbf{q}) \mathcal{M}_j(\mathbf{q})| \right). \quad (18)
\end{aligned}$$

We now bound each term individually. Consider the terms $j \neq s$ first. Since $0 \leq \mathcal{M}_s(\mathbf{q}) \leq 1$, we can bound them as

$$|k_s^i \mathcal{M}_s(\mathbf{q}) \mathcal{M}_j(\mathbf{q})| \leq |k_s^i|. \quad (19)$$

Now recall that the inequality $ab \leq (a+b)^2/4$ holds for any real numbers a and b with equality holding at $a = b$. Therefore, for the first term, we obtain

$$|k_j^i (1 - \mathcal{M}_j(\mathbf{q})) \mathcal{M}_j(\mathbf{q})| \leq |k_j^i| \frac{(1 - \mathcal{M}_j(\mathbf{q}) + \mathcal{M}_j(\mathbf{q}))^2}{4} = \frac{|k_j^i|}{4}. \quad (20)$$

Combining 18, 19 and 20, we finally arrive at

$$|\mathbf{J}_{\mathcal{M}(\mathbf{q})_{ji}}| = \left| \frac{\partial}{\partial q^i} \mathcal{M}_j(\mathbf{q}) \right| \leq m_i \left(\frac{|k_j^i|}{4} + \sum_{s \in [N] \setminus \{j\}} |k_s^i| \right) = \kappa_{ij} m_i \quad (21)$$

for all $i \in [D]$ and $j \in [N]$, where $\kappa_{ij} \geq 0$ denotes the coefficient in the bracket. \square

B.2 Proof of Proposition 1

Let us estimate the distance between two output vectors of Elliptical attention mechanism corresponding to clean and contaminated query inputs, namely:

$$\begin{aligned}\mathbf{h} &= \sum_{j \in [N]} \text{softmax}(\mathbf{q}^\top \mathbf{M} \mathbf{k}_j / \sigma^2) \mathbf{v}_j = \sum_{j \in [N]} \mathcal{M}_j(\mathbf{q}) \mathbf{v}_j \\ \mathbf{h}_\epsilon &= \sum_{j \in [N]} \text{softmax}((\mathbf{q} + \boldsymbol{\epsilon})^\top \mathbf{M} \mathbf{k}_j / \sigma^2) \mathbf{v}_j = \sum_{j \in [N]} \mathcal{M}_j(\mathbf{q} + \boldsymbol{\epsilon}) \mathbf{v}_j,\end{aligned}$$

where \mathcal{M} is defined as in Lemma 1. We omit the keys and scaling parameter for convenience since they do not affect the analysis. Then,

$$\begin{aligned}\|\mathbf{h} - \mathbf{h}_\epsilon\| &= \left\| \sum_{j \in [N]} (\mathcal{M}_j(\mathbf{q}) - \mathcal{M}_j(\mathbf{q} + \boldsymbol{\epsilon})) \mathbf{v}_j \right\| \\ &\leq \sum_{j \in [N]} |\mathcal{M}_j(\mathbf{q}) - \mathcal{M}_j(\mathbf{q} + \boldsymbol{\epsilon})| \|\mathbf{v}_j\| \\ &\leq \sum_{j \in [N]} \|\nabla \mathcal{M}_j(\hat{\mathbf{q}})\| \|\boldsymbol{\epsilon}\| \|\mathbf{v}_j\| \tag{22}\end{aligned}$$

$$\begin{aligned}&= \sum_{j \in [N]} \sqrt{\sum_{i \in [D]} (\mathbf{J}_{\mathcal{M}}(\hat{\mathbf{q}})_{ji})^2} \|\mathbf{v}_j\| \|\boldsymbol{\epsilon}\| \\ &\leq \sum_{j \in [N]} \sqrt{\sum_{i \in [D]} \kappa_{ij}^2 m_i^2} \|\mathbf{v}_j\| \|\boldsymbol{\epsilon}\| \tag{23} \\ &= \sum_{j \in [N]} \sqrt{\text{tr}(\mathbf{K}_j^2 \mathbf{M}^2)} \|\mathbf{v}_j\| \|\boldsymbol{\epsilon}\|,\end{aligned}$$

where $\mathbf{K}_j := \text{diag}(\kappa_{1j}, \kappa_{2j}, \dots, \kappa_{Dj})$ and κ_{ij} is defined as in Eqn. 21. Note that 22 follows from mean value theorem for some $\beta \in [0, 1]$ and $\hat{\mathbf{q}} := \mathbf{q} + \beta \boldsymbol{\epsilon}$ while 23 follows from Lemma 1. \square

B.3 Proof of Proposition 2

Let the output at layer ℓ be denoted as \mathbf{h}^ℓ , the standard self-attention estimator and Elliptical estimator fitted at layer ℓ be denoted \hat{f}^ℓ and \hat{f}_d^ℓ respectively, where d is the Mahalanobis metric described in Eqn. 7, and f be the true underlying function described in Eqn. 3. By assumption, \hat{f} is a higher variance estimator than \hat{f}_d for any layer. The output for either estimator at layer ℓ can be decomposed into ground truth and noise as follows:

$$\mathbf{h}^\ell = \hat{f}^\ell(\mathbf{q}^\ell) = f(\mathbf{q}^\ell) + \boldsymbol{\epsilon}^\ell \tag{24}$$

$$\mathbf{h}_d^\ell = \hat{f}_d^\ell(\mathbf{q}^\ell) = f(\mathbf{q}^\ell) + \boldsymbol{\eta}^\ell, \tag{25}$$

where $\boldsymbol{\eta}^\ell \sim \gamma(\mathbf{0}, V_\eta)$, $\boldsymbol{\epsilon}^\ell \sim \gamma(\mathbf{0}, V_\epsilon)$ are the noise components of the estimate at \mathbf{q}^ℓ and $f(\mathbf{q}^\ell)$ is the ground truth. By assumption of \hat{f}_d being lower variance, $V_\epsilon - V_\eta$ is a positive semi-definite matrix.

We first require the following Assumption 1, which is described as:

Assumption 1 (Random Input Noise Causes Estimator Attenuation) . Let \hat{f} be any estimator of true function f and let the input $\mathbf{x} \sim \mu$ drawn from marginal μ be randomly corrupted by random noise $\epsilon \sim (0, V)$ of some unknown distribution and variance matrix V . Let \mathbf{c} be some constant. Then, random input noise attenuates the estimator as follows:

$$\mathbb{E}_{\mathbf{x} \sim \mu} \|\hat{f}(\mathbf{x} + \epsilon) - \mathbf{c}\| \leq \mathbb{E}_{\mathbf{x} \sim \mu} \|\hat{f}(\mathbf{x}) - \mathbf{c}\| \quad (26)$$

Assumption 1 is a well-studied phenomenon in parametric regression, often referred to as attenuation bias [60], regression dilution [14], or errors-in-variables [29]. In parametric regression, it can be shown to have an exact form where the estimated gradients of the model are attenuated towards 0 proportional to the variance of the noise ϵ . In non-parametric regression, addition of input noise is often referred to as random smoothing or random input smoothing [41, 7], and is well known to be used as regularization technique to introduce bias into the model. In non-parametric models, no exact closed forms exist to express the attenuation bias, but for our purposes we only note the attenuation exists and provide a general form of it in Assumption 1.

The outputs of 24 and 25 then become the inputs to the following layer after being self-added, normalized, projected, and linearly transformed. For notational simplicity and because these operations do not change the analysis, we denote the input at the next layer as the previous layer output $\mathbf{q}^{\ell+1} = \mathbf{h}^\ell$. We therefore have the following process:

$$\mathbf{h}^{\ell+1} = \hat{f}^{\ell+1}(\mathbf{q}^{\ell+1}) = \hat{f}^{\ell+1}(\mathbf{h}^\ell) = \hat{f}^{\ell+1}(\underbrace{f(\mathbf{q}^\ell) + \epsilon^\ell}_{\mathbf{z}^\ell}), \quad (27)$$

where we see the output $\mathbf{h}^{\ell+1}$ is obtained by fitting $\hat{f}^{\ell+1}$ to input \mathbf{z}^ℓ which is composed of ground truth $f(\mathbf{q}^\ell)$ and noise ϵ^ℓ passed through from the previous layer.

The result then follows directly from the fact that in any given layer, the standard self-attention estimator produces noisier estimates, where that noise is then passed into the subsequent layer as input noise. This is

$$\mathbb{E} \|\mathbf{h}^{\ell+1} - \mathbf{c}\| = \mathbb{E} \|\hat{f}^{\ell+1}(\mathbf{q}^{\ell+1}) - \mathbf{c}\| = \mathbb{E} \|\hat{f}^{\ell+1}(f(\mathbf{q}^\ell) + \epsilon^\ell) - \mathbf{c}\| \quad (28)$$

$$\leq \mathbb{E} \|\hat{f}^{\ell+1}(f(\mathbf{q}^\ell) + \eta^\ell) - \mathbf{c}\| \quad (29)$$

$$\approx \mathbb{E} \|\hat{f}_d^{\ell+1}(f(\mathbf{q}^\ell) + \eta^\ell) - \mathbf{c}\| \quad (30)$$

$$= \mathbb{E} \|\hat{f}_d^{\ell+1}(f(\mathbf{q}^{\ell+1})) - \mathbf{c}\| = \mathbb{E} \|\mathbf{h}_d^{\ell+1} - \mathbf{c}\|, \quad (31)$$

where line 29 follows from combining the fact that η^ℓ is lower variance with Assumption 1 and line 30 follows from the fact that $\mathbb{E} \|X\| \approx \mathbb{E} \|Y\|$ when X, Y have the same mean and roughly similar distribution.

Therefore we obtain at any layer ℓ the following

$$\mathbb{E} \|\mathbf{h}^{\ell+1} - \mathbf{c}\| \leq \mathbb{E} \|\mathbf{h}_d^{\ell+1} - \mathbf{c}\|, \quad (32)$$

as required. \square

B.4 Proof of Proposition 3

The lemma below encapsulates the necessary calculations that will then be used in the following proofs.

Lemma 2 *Given a normally distributed zero mean random variable $\xi \sim \mathcal{N}(0, \sigma^2)$, the expectation of a random variable obtained by its absolute value is $\mathbb{E}|\xi| = \sqrt{2\sigma^2/\pi}$.*

Proof. Since $\xi \sim \mathcal{N}(0, \sigma^2)$, by definition of expectation, we have

$$\begin{aligned} \mathbb{E}|\xi| &= \int_{-\infty}^{\infty} \frac{|x|}{\sqrt{2\pi\sigma^2}} \exp\left(-\frac{x^2}{2\sigma^2}\right) dx \\ &= \int_{-\infty}^0 \frac{-x}{\sqrt{2\pi\sigma^2}} \exp\left(-\frac{x^2}{2\sigma^2}\right) dx + \int_0^{\infty} \frac{x}{\sqrt{2\pi\sigma^2}} \exp\left(-\frac{x^2}{2\sigma^2}\right) dx \end{aligned} \quad (33)$$

$$\begin{aligned} &= \frac{2}{\sqrt{2\pi\sigma^2}} \int_0^{\infty} x \exp\left(-\frac{x^2}{2\sigma^2}\right) dx \\ &= \sqrt{\frac{2}{\pi\sigma^2}} \left[-\sigma^2 \exp\left(-\frac{x^2}{2\sigma^2}\right) \right]_0^{\infty} \\ &= \sqrt{\frac{2\sigma^2}{\pi}}, \end{aligned} \quad (34)$$

where we used the variable change $x \leftarrow (-x)$ in the first integral of 33 to obtain 34. \square

We derive the bounds for the impact of noise in 3, with respect to its variance, on our estimator 12 in Lemma 3. Henceforth, we omit the factor δ in Eqn. 12 since it does not affect the further analysis.

Lemma 3 *Given that the noise term in 3 follows a normal distribution with zero mean and variance σ^2 , the following inequality*

$$\left| m_i - \mathbb{E}|f_i(\mathbf{k}^{\ell+1}) - f_i(\mathbf{k}^{\ell})| \right| \leq \frac{2}{\sqrt{\pi}}\sigma \quad (35)$$

holds for all $i \in [D]$, where f_i denotes the i^{th} component of $f(\mathbf{k}^{\ell}) = (f_1(\mathbf{k}), f_2(\mathbf{k}), \dots, f_D(\mathbf{k}))^{\top}$.

Proof. Since all value vectors are taken from the data generating process 3, we have

$$\begin{aligned} m_i &= \mathbb{E}_{(\mathbf{v}^{\ell}, \mathbf{v}^{\ell+1}) \in \mathcal{X}_v^{\ell, \ell+1}} |\mathbf{v}_i^{\ell+1} - \mathbf{v}_i^{\ell}| \\ &= \mathbb{E}|f_i(\mathbf{k}^{\ell+1}) - f_i(\mathbf{k}^{\ell}) + \epsilon_i^{\ell+1} - \epsilon_i^{\ell}|, \end{aligned} \quad (36)$$

where ϵ_i^{ℓ} and $\epsilon_i^{\ell+1}$ denote the i^{th} components of the noise terms $\boldsymbol{\epsilon}^{\ell}$ and $\boldsymbol{\epsilon}^{\ell+1}$, respectively. Note that for real numbers a and b , we have by triangle inequality that $|a + b| \leq |a| + |b|$ and $|a + b| = |a - (-b)| \geq ||a| - |-b|| \geq |a| - |b|$. Applying these and the linearity of expectation to 36, we obtain

$$\mathbb{E}|f_i(\mathbf{k}^{\ell+1}) - f_i(\mathbf{k}^{\ell})| - \mathbb{E}|\epsilon_i^{\ell+1} - \epsilon_i^{\ell}| \leq m_i \leq \mathbb{E}|f_i(\mathbf{k}^{\ell+1}) - f_i(\mathbf{k}^{\ell})| + \mathbb{E}|\epsilon_i^{\ell+1} - \epsilon_i^{\ell}| \quad (37)$$

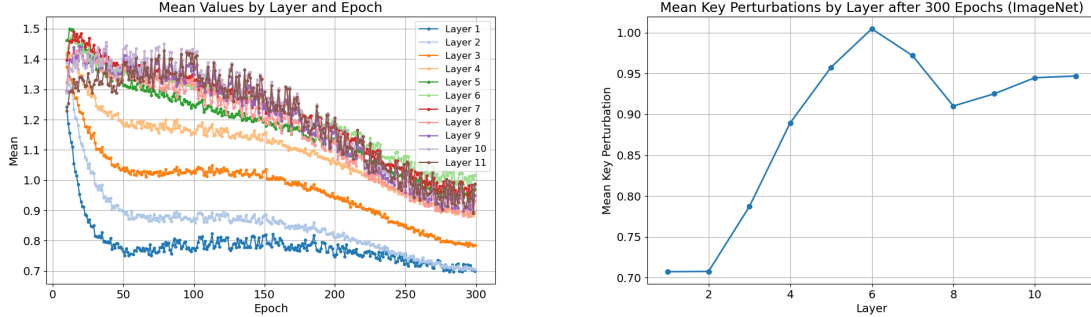


Figure 5: **Left:** Evolution of mean values of key perturbations over successive layers. **Right:** Mean key perturbations at different layers after 300 epochs. The figures show that as the number of layers increases, mean key perturbations over layers stabilize around a constant value.

Recall that $\epsilon_i^\ell \sim \mathcal{N}(0, \sigma^2)$ and independent. Now we have that $\epsilon_i^{\ell+1} - \epsilon_i^\ell \sim \mathcal{N}(0, 2\sigma^2)$ as the mean value does not change while variance accumulates when subtracting two zero-mean normal variables. Therefore, the Lemma 2 gives that

$$\mathbb{E}|\epsilon_i^{\ell+1} - \epsilon_i^\ell| = \frac{2}{\sqrt{\pi}}\sigma.$$

Plugging this back into the inequalities 37, we get

$$\mathbb{E}|f_i(\mathbf{k}^{\ell+1}) - f_i(\mathbf{k}^\ell)| - \frac{2}{\sqrt{\pi}}\sigma \leq m_i \leq \mathbb{E}|f_i(\mathbf{k}^{\ell+1}) - f_i(\mathbf{k}^\ell)| + \frac{2}{\sqrt{\pi}}\sigma,$$

which is equivalent to 35 as desired. \square

Proof of Proposition 3. We shall first make the following assumptions on the data generating process 3:

Assumption 2 *The underlying coordinate system in the feature space \mathcal{X}_k is independent, implying that the function $f : \mathbb{R}^D \rightarrow \mathbb{R}^D$ in Eqn. 3 can be separated as $f(\mathbf{k}) = (f_1(k_1), \dots, f_D(k_D))^\top$*

Assumption 3 *The noise term in Eqn. 3 has independent components with each component ϵ_j^ℓ following a normal distribution $\mathcal{N}(0, \sigma^2)$ for small σ , for all $j \in [D]$ and $\ell \in \mathbb{N}$*

Assumption 4 *The magnitude of each component of key perturbations across consecutive layers, defined as $|k_i^{\ell+1} - k_i^\ell|$, follows a distribution with small, layer-independent mean (δ) and variance (ν)*

Remark 6 *The assumption of layer-independence in Assumption 4, especially for deeper layers, is supported well empirically, as shown in Figure 5. Given the over-smoothing observed in transformers [61], where token representations stabilize after initial few layers, it is also practical to assume that key perturbations across layers have relatively small mean and variance when modelled as a random process.*

Proof. Under the Assumptions 2, 3, 4, we show that $\|f'_i\|_{1,\mu} \geq \|f'_j\|_{1,\mu}$ implies $m_i \geq m_j$ with high probability where m_i is defined as in 12.

Directly from the Lemma 3, we have

$$\left| m_i - \mathbb{E}|f_i(\mathbf{k}^{\ell+1}) - f_i(\mathbf{k}^\ell)| \right| \leq \frac{2}{\sqrt{\pi}}\sigma.$$

Letting $\sigma \rightarrow 0$ in this inequality, which is feasible under the Assumption 3, one can get with a small error that

$$m_i \approx \mathbb{E}|f_i(\mathbf{k}^{\ell+1}) - f_i(\mathbf{k}^\ell)|, \quad (38)$$

which in turn implies that the impact of the noise in 12 is negligible and the error of ignoring them can be controlled by the bounds given by 35. Now according to the theorem statement,

$$\begin{aligned} \|f'_i\|_{1,\mu} \geq \|f'_j\|_{1,\mu} &\iff \mathbb{E}\|\mathbf{J}_f(\mathbf{k})\mathbf{e}_i\|_1 \geq \mathbb{E}\|\mathbf{J}_f(\mathbf{k})\mathbf{e}_j\|_1 \\ &\iff \mathbb{E}\left[\sum_{s \in [D]} \left|\frac{\partial f_s(\mathbf{k})}{\partial k_i}\right|\right] \geq \mathbb{E}\left[\sum_{s \in [D]} \left|\frac{\partial f_s(\mathbf{k})}{\partial k_j}\right|\right] \\ &\iff \mathbb{E}|f'_i(k_i)| \geq \mathbb{E}|f'_j(k_j)| \end{aligned} \quad (39)$$

where we used the separability of f as given in Assumption 2 which simplifies the Jacobian matrix as

$$\begin{aligned} \mathbf{J}_f(\mathbf{k}) &= \begin{bmatrix} \frac{\partial f_1(\mathbf{k})}{\partial k_1} & \frac{\partial f_1(\mathbf{k})}{\partial k_2} & \cdots & \frac{\partial f_1(\mathbf{k})}{\partial k_D} \\ \frac{\partial f_2(\mathbf{k})}{\partial k_1} & \frac{\partial f_2(\mathbf{k})}{\partial k_2} & \cdots & \frac{\partial f_2(\mathbf{k})}{\partial k_D} \\ \vdots & \vdots & \ddots & \vdots \\ \frac{\partial f_D(\mathbf{k})}{\partial k_1} & \frac{\partial f_D(\mathbf{k})}{\partial k_2} & \cdots & \frac{\partial f_D(\mathbf{k})}{\partial k_D} \end{bmatrix} = \begin{bmatrix} \frac{\partial f_1(k_1)}{\partial k_1} & \frac{\partial f_1(k_1)}{\partial k_2} & \cdots & \frac{\partial f_1(k_1)}{\partial k_D} \\ \frac{\partial f_2(k_2)}{\partial k_1} & \frac{\partial f_2(k_2)}{\partial k_2} & \cdots & \frac{\partial f_2(k_2)}{\partial k_D} \\ \vdots & \vdots & \ddots & \vdots \\ \frac{\partial f_D(k_D)}{\partial k_1} & \frac{\partial f_D(k_D)}{\partial k_2} & \cdots & \frac{\partial f_D(k_D)}{\partial k_D} \end{bmatrix} \\ &= \begin{bmatrix} f'_1(k_1) & 0 & \cdots & 0 \\ 0 & f'_2(k_2) & \cdots & 0 \\ \vdots & \vdots & \ddots & \vdots \\ 0 & 0 & \cdots & f'_D(k_D) \end{bmatrix}, \end{aligned}$$

so that $[\mathbf{J}_f(\mathbf{k})]_{ii} = f'_i(k_i)$. Using the definition of derivative, the inequality 39 is equivalent to

$$\mathbb{E}\left|\lim_{\tau \rightarrow 0} \frac{f^i(k_i^\ell + \tau) - f^i(k_i^\ell)}{\tau}\right| \geq \mathbb{E}\left|\lim_{\tau \rightarrow 0} \frac{f^j(k_j^\ell + \tau) - f^j(k_j^\ell)}{\tau}\right|. \quad (40)$$

Next, we note that for a small δ , the limits in 40 can be approximated with $\frac{f^s(k_s^\ell + \delta) - f^s(k_s^\ell)}{\delta}$ for $s \in \{i, j\}$:

$$\frac{\mathbb{E}|f^i(k_i^\ell + \delta) - f^i(k_i^\ell)|}{\delta} \geq \frac{\mathbb{E}|f^j(k_j^\ell + \delta) - f^j(k_j^\ell)|}{\delta}. \quad (41)$$

Let us choose $\delta = \mathbb{E}|k_i^{\ell+1} - k_i^\ell|$. Then, by Chebyshev's inequality, we have for any $\varepsilon > 0$ that

$$\begin{aligned} 1 - \frac{\nu^2}{\varepsilon^2} &\leq \mathbb{P}\left(\left||k_i^{\ell+1} - k_i^\ell| - \delta\right| \leq \varepsilon\right) \\ &= \mathbb{P}\left(\delta - \varepsilon \leq |k_i^{\ell+1} - k_i^\ell| \leq \delta + \varepsilon\right). \end{aligned} \quad (42)$$

Given that the variance ν is sufficiently small as in the Assumption 4, the inequality 42 implies that $k_i^{\ell+1} \approx k_i^\ell \pm \delta$ with high probability. Therefore, it follows from 41 with high probability that

$$\frac{\mathbb{E}|f^i(k_i^{\ell+1}) - f^i(k_i^\ell)|}{\delta} \geq \frac{\mathbb{E}|f^j(k_j^{\ell+1}) - f^j(k_j^\ell)|}{\delta},$$

which, due to 38, is equivalent to $m_i \geq m_j$ as desired. \square

B.5 Lipschitz smoothness in (\mathcal{X}, d)

Below we show how Lipschitz smoothness of f changes when moving from Euclidean to the Mahalanobis transformed space. We shall follow similar steps to [24] and [25] but for a more general class of functions.

Proposition 4 (Change in Lipschitz smoothness for f) *Suppose there exists a positive constant G_i such that $\|\nabla f_i(\mathbf{k})\| \leq G_i$ for any $\mathbf{k} \in \mathcal{X}_{\mathbf{k}}$ and $m_i > 0$ for all $i \in [D]$. Then for any $\mathbf{q}, \mathbf{k} \in \mathcal{X}_{\mathbf{k}}$, the following inequality holds:*

$$\|f(\mathbf{q}) - f(\mathbf{k})\| \leq \left(\sum_{i \in [D]} \frac{G_i}{\sqrt{m_i}} \right) d(\mathbf{q}, \mathbf{k}).$$

Proof. Let $\boldsymbol{\omega} := \frac{\mathbf{q} - \mathbf{k}}{\|\mathbf{q} - \mathbf{k}\|}$ denote the unit vector pointing from \mathbf{k} to \mathbf{q} . The fundamental theorem of calculus implies that

$$f(\mathbf{q}) - f(\mathbf{k}) = \int_0^{\|\mathbf{q} - \mathbf{k}\|} \frac{d}{dt} f(\mathbf{k} + t\boldsymbol{\omega}) dt = \int_0^{\|\mathbf{q} - \mathbf{k}\|} \boldsymbol{\omega}^\top \mathbf{J}_f(\mathbf{k} + t\boldsymbol{\omega}) dt,$$

where \mathbf{J}_f is the Jacobian matrix of f as usual. Starting with the distance between outputs $f(\mathbf{q})$ and $f(\mathbf{k})$ we have

$$\begin{aligned} \|f(\mathbf{q}) - f(\mathbf{k})\| &= \left\| \int_0^{\|\mathbf{q} - \mathbf{k}\|} \boldsymbol{\omega}^\top \mathbf{J}_f(\mathbf{k} + t\boldsymbol{\omega}) dt \right\| \leq \int_0^{\|\mathbf{q} - \mathbf{k}\|} \left\| \sum_{i \in [D]} \omega_i \nabla f_i(\mathbf{k} + t\boldsymbol{\omega}) \right\| dt \\ &\leq \int_0^{\|\mathbf{q} - \mathbf{k}\|} \sum_{i \in [D]} |\omega_i| \|\nabla f_i(\mathbf{k} + t\boldsymbol{\omega})\| dt \leq \sum_{i \in [D]} G_i |\omega_i| \int_0^{\|\mathbf{q} - \mathbf{k}\|} dt \\ &= \sum_{i \in [D]} G_i |q_i - k_i|, \end{aligned} \quad (43)$$

where, as for all other vectors, q_i denotes the i^{th} component of vector \mathbf{q} . Now note that

$$|q_i - k_i| \leq \sqrt{(q_i - k_i)^2 + \sum_{j \neq i} \frac{m_j}{m_i} (q_j - k_j)^2} = \sqrt{\frac{(\mathbf{q} - \mathbf{k})^\top \mathbf{M}(\mathbf{q} - \mathbf{k})}{m_i}} = \frac{d(\mathbf{q}, \mathbf{k})}{\sqrt{m_i}}. \quad (44)$$

Combining 43 and 44, we finally attain

$$\|f(\mathbf{q}) - f(\mathbf{k})\| \leq \sum_{i \in [D]} \frac{G_i}{\sqrt{m_i}} d(\mathbf{q}, \mathbf{k}), \quad (45)$$

which completes the proof. \square

C Additional Theorems

The following Theorem 1 is a classic result from [62]. We refer the reader to their work for details.

Theorem 1 (Minimax rate for functions of bounded variability [62]) *Let F_λ denote the class of distributions $P_{X,Y}$ on $\mathcal{X} \times [0, 1]$ such that $\forall i \in [d]$, the directional derivatives of $f(x) := \mathbb{E}[Y|X = x]$ satisfy $|f'_i|_{\text{sup}} := \sup_{\mathbf{q} \in \mathcal{X}_k} \|\nabla f_i(\mathbf{q})\|_{\text{sup}} \leq \lambda$. Then for any $f \in F_\lambda$, estimator \hat{f} , sample size $n \in \mathbb{N}$, there exists a $\tilde{c} \leq 1$ independent of n satisfying*

$$\inf_{f_n} \sup_{f \in \mathcal{F}_\lambda} \mathbb{E}_{X^n, Y^n} \|\hat{f} - f\|^2 \geq 2\tilde{c}^{2/(2+d)} (d\lambda)^{2d/(2+d)} n^{-2/(2+d)} \quad (46)$$

Theorem 2 (Improvement in MSE for approximately sparse functions [25]) *Let the norm of the largest gradient be $\lambda := \sup_{i \in [D]} \|\nabla f_i(\mathbf{q})\|_{\text{sup}}$ and \hat{f}_d be an estimator in metric space (\mathcal{X}_q, d) where d is defined as Eqn. 7. Then,*

$$\mathbb{E} \|\hat{f}_d - f\|_2^2 < \inf_{\tilde{f}} \sup_{\mathcal{F}_\lambda} \mathbb{E} \|\tilde{f} - f\|_2^2. \quad (47)$$

Proof. We provide an abridged proof for completeness. We refer the reader to [25] for the full details.

First, the full bound is described as follows:

$$\mathbb{E} \|\hat{f}_d - f\|_2^2 \leq 2C_{\kappa_R}^{2/2+r} (CD\lambda_d d(\mathcal{X}))^{2r/2+r} n^{-2/2+r} < \inf_{\tilde{f}} \sup_{\mathcal{F}_\lambda} \mathbb{E} \|\tilde{f} - f\|_2^2, \quad (48)$$

where $d(\mathcal{X})$ is the d-diameter of \mathcal{X} defined as $\sup_{x, x' \in \mathcal{X}} d(x, x')$, $R \subset [D]$, $1 \leq C_{\kappa_R} \leq C'(4\kappa_R)^{|R|}$, C and C_1 are universal constants and $\lambda_d \geq \sup_i \|f'_i\|_{\text{sup}} / \sqrt{m_i}$. Let

$$r(\epsilon) \leq \begin{cases} |R| & \text{if } \epsilon \geq \epsilon_R/d(\mathcal{X}) \\ D - (D - |R|) \frac{\log(d(\mathcal{X})/\epsilon_R)}{\log(1/\epsilon)} & \text{if } \epsilon < \epsilon_R/d(\mathcal{X}) \end{cases}.$$

For bandwidth ϵ_n , $r = r(\epsilon_n)$ and let $|R| \leq r \leq D$. Let $\epsilon > 0$, \tilde{c} be defined as the same \tilde{c} in Theorem 1, and $n \in \mathbb{N}$, define the function $\psi_{n,d} = C\epsilon^{-r(\epsilon)}/n$ and $\psi_{n,d}(\epsilon) = C_1\epsilon^{-D}/n$ where $C_1 = \tilde{c}(\lambda/C\lambda_d d(\mathcal{X}))^D$. Also define $\phi(\epsilon) = C^2 D^2 \lambda_d^2 d(\mathcal{X})^2 \cdot \epsilon^2$.

For any fixed n , let $\epsilon_{n,d}$ be a solution to $\psi_{n,d}(\epsilon) = \phi(\epsilon)$. Solving for $\epsilon_{n,d}$ obtains the following lower bound on the minmax rate of

$$2\phi(\epsilon_{n,d}) = 2\tilde{c}^{2/(2+D)}(D\lambda)^{2d/(2+d)}n^{-2/(2+d)}. \quad (49)$$

For any $n \in \mathbb{N}$ there exists a solution $\epsilon_{n,d}$ to the equation $\psi_{n,d}(\epsilon) = \phi(\epsilon)$ since $r(\epsilon)$ is nondecreasing. Therefore it is possible to obtain the following:

$$\mathbb{E}_{X^n, Y^n} \|f_{n,\epsilon,d} - f\|_2^2 \leq 2\phi(\epsilon_{n,d}). \quad (50)$$

Since ϕ is independent of n , and both $\psi_{n,d}$ and $\psi_{n,d}$ are strictly decreasing functions of n , we have that $\epsilon_{n,d}$ and $\epsilon_{n,d}$ both tend to 0 as $n \rightarrow \infty$. Therefore we can define n_0 such that, for all $n \geq n_0$, both $\epsilon_{n,d}$ and $\epsilon_{n,d}$ are less than $\epsilon_{\mathcal{R}}/d(\mathcal{X})$.

Thus, $\forall n \geq n_0$, we have $\epsilon_{n,d} < \epsilon_{n,d}$ if, for all $0 < \epsilon < \epsilon_{\mathcal{R}}/d(\mathcal{X})$, $\psi_{n,d}(\epsilon) < \psi_{n,d}(\epsilon)$, which completes the proof \square .

D A Consistent Estimator

In this section, we present a consistent centered difference-based quotient estimator of the coordinate-wise variability obtained by perturbing the estimated function in the i^{th} direction and measuring the L_1 norm of the difference. Similarly, this estimator requires no learnable parameters or gradients. The estimator is described in the following proposition.

Proposition 5 (Consistent Estimator) *Given a function $f : \mathbb{R}^D \rightarrow \mathbb{R}^{D_v}$ with i^{th} directional variation $\|f'_i\|_{1,\mu}$, $i \in [D]$, the directional variation can be estimated by the quantity*

$$\hat{m}_i := \mathbb{E}_n \left[\frac{\|\bar{f}(\mathbf{k} + t\mathbf{e}_i) - \bar{f}(\mathbf{k} - t\mathbf{e}_i)\|_1}{2t} \right], \quad (51)$$

where t is a hyperparameter controlling the degree of locality of the estimator and \mathbb{E}_n denotes the empirical expectation for n samples.

Despite \hat{m}_i in proposition 5's simple formulation, it is nonetheless a consistent estimator of the coordinate-wise variation in the underlying function. We utilize a simplified version of a theorem from [25], adapted to suit our specific needs, as the original formulation is more detailed than necessary for our purposes.

Theorem 3 (Consistency of Centered Difference-based Estimator for Scalar Function [25])

Let $\varphi : \mathbb{R}^D \rightarrow \mathbb{R}$ be a smooth scalar function and $\|\varphi'_i\|_{1,\mu} := \mathbb{E}_{\mathbf{x} \sim \mu} |\mathbf{e}_i^\top \nabla \varphi|$ be the coordinate-wise variability for that scalar function. Then, for any direction i and any $0 < \delta < 1/2$, the following bound holds with probability of at least $1 - 2\delta$:

$$\left| \mathbb{E}_n \frac{|\bar{\varphi}(\mathbf{x} + t\mathbf{e}_i) - \bar{\varphi}(\mathbf{x} - t\mathbf{e}_i)|}{2t} - \|\varphi'_i\|_{1,\mu} \right| \leq \mathcal{O}(n^{-1/2}t^{-1} \ln(2D/\delta)^{1/2}). \quad (52)$$

Note that the Theorem 3 is different from our setting by studying a scalar function as opposed to a vector valued function. However, we show that the result can be generalized to the latter case in Corollary 1 below via the estimator 51.

Corollary 1 (Consistency of the Estimator (51) for Vector-valued Function) *Let $f : \mathbb{R}^D \rightarrow \mathbb{R}^{D_v}$ be a vector valued function and $\|f'_i\|_{1,\mu}$ be defined as in Definition 1. Then, for any direction i and any $0 < \delta < 1/2$, the following bound holds with probability of at least $1 - 2\delta$:*

$$|\widehat{m}_i - \|f'_i\|_{1,\mu}| \leq \mathcal{O}(n^{-1/2}t^{-1} \ln(2D/\delta)^{1/2}). \quad (53)$$

Proof. We first derive the relation between the left hand side of 53 and its coordinate-wise differences as follows:

$$\begin{aligned} |\widehat{m}_i - \|f'_i\|_{1,\mu}| &= \left| \mathbb{E}_n \left[\frac{\|\bar{f}(\mathbf{k} + te_i) - \bar{f}(\mathbf{k} - te_i)\|_1}{2t} \right] - \mathbb{E}_{\mathbf{k} \sim \mu} [\|\mathbf{J}_f(\mathbf{k})\mathbf{e}_i\|_1] \right| \\ &= \left| \mathbb{E}_n \left[\sum_{j \in [D]} \frac{|\bar{f}_j(\mathbf{k} + te_i) - \bar{f}_j(\mathbf{k} - te_i)|}{2t} \right] - \mathbb{E}_{\mathbf{k} \sim \mu} \left[\sum_{j \in [D]} |\mathbf{e}_i^\top \nabla f_j| \right] \right| \end{aligned} \quad (54)$$

$$= \left| \sum_{j \in [D]} \mathbb{E}_n \frac{|\bar{f}_j(\mathbf{k} + te_i) - \bar{f}_j(\mathbf{k} - te_i)|}{2t} - \sum_{j \in [D]} \mathbb{E}_{\mathbf{k} \sim \mu} |\mathbf{e}_i^\top \nabla f_j| \right| \quad (55)$$

$$= \left| \sum_{j \in [D]} \left(m_i^{(j)} - \|f'_i\|_{1,\mu}^{(j)} \right) \right| \quad (\text{definition of } m_i \text{ and } \|f'_i\|_{1,\mu} \text{ for components } f_j)$$

$$\leq \sum_{j \in [D]} \left| m_i^{(j)} - \|f'_i\|_{1,\mu}^{(j)} \right| \quad (\text{triangle inequality})$$

$$\leq \mathcal{O}(n^{-1/2}t^{-1} \ln(2D/\delta)^{1/2}), \quad (\text{Theorem 3})$$

where line 54 follows from the definition of the ℓ_1 norm, line 55 follows from the linearity of expectation, the superscript j indicates that the case is reduced to the scalar function case for each j^{th} summand individually. Note that the probability of the last bound is at least $(1 - 2\delta/D)^D$ since each component-wise bound holds with probability at least $1 - 2\delta/D$. However, since we can choose δ small enough such that $2\delta < 1$, by Bernoulli's inequality $(1 - 2\delta/D)^D \geq 1 - 2D\delta/D = 1 - 2\delta$. \square

Remark 7 *Despite the proven consistency of this estimator, we opt for the efficient estimator presented in our main body described in Eqn 12. This is because the consistent estimator requires materialising the prediction function – that is, computing a forward pass of the self-attention mechanism – twice per dimension. This makes the consistent estimator unusable in most problem settings. We present results for the consistent estimator in Appendix F.8.*

E Implementation Procedure and Computational Efficiency

Training and Inference. Given Elliptical Attention requires keys and values from the previous layer in order to compute the required transformation, we can only implement Elliptical Attention from the second layer on. We incorporate our Elliptical Attention into both training and inference stages. This is because, firstly, Elliptical Attention is designed to offer improvements to both clean and contaminated data, and so even in the presence of completely clean train and test data, it is advantageous to incorporate Elliptical Attention into

both stages. Secondly, it is commonplace to encounter data contamination in test data and indeed also highly possible to encounter it in train data as well. Therefore, in the interest of robustness as well, we also incorporate Elliptical Attention into both stages.

Computational Efficiency. Computing the required transformation requires no learnable parameters and is obtained simply by averaging absolute differences in values over layers. These operations are therefore just of the order $\mathcal{O}(bhnD) = \mathcal{O}(n)$ for batch size b , head number h , key/value length n , and dimension D . Hence upper-bound time complexity of the overall Transformer is unaffected. We provide efficiency analysis in terms of computation speed and max GPU memory allocated (calculated by CUDA `max_memory_allocated` in Figure 4, which shows that compared with baseline robust models, Elliptical is the fastest and most memory efficient. Elliptical exhibits no perceptible slowdown versus DeiT of the same configuration and only a 0.99% increase in max memory allocated, which is why Elliptical and DeiT are shown as the same data point in the Figure 4.

F Experimental Details and Additional Experiments

F.1 Out-of-Distribution Robustness and Data Corruption on ImageNet-A,R,C

ImageNet-A,R,C are benchmarks capturing a range of out-of-distribution and corrupted samples. ImageNet-A contains real world adversarially filtered images that fool current ImageNet classifiers. ImageNet-R contains various artistic renditions of object classes from the original ImageNet. ImageNet-C consists of 15 types of algorithmically generated corruptions with 5 levels of severity (e.g blurring, pixelation, speckle noise etc). Given that Elliptical Attention learns attention weights dependant on the transformation \mathbf{M} , which is itself dependant on the train data distribution, our proposed model is not designed for situations in which the test distribution is substantially different from the train distribution. This then includes OOD robustness and robustness to heavy corruption to the point where the underlying data distribution is fundamentally different. We nonetheless evaluate Elliptical Attention on ImageNet-A,R,C to assess these important forms of robustness as well. Table 7 shows that Elliptical Attention is still able to offer improvements over baseline *DeiT* in terms of OOD robustness, while maintaining approximately the same performance as the baseline for ImageNet-C. Figure 7 shows for *Fog* and *Pixelate* corruptions how Elliptical compares with DeiT over the 5 severity levels, where we see that at low severity levels Elliptical improves over DeiT, however as the severity level gets too high Elliptical falls behind. This agrees with our expectation that as the severity level grows, the distribution is further shifted relative to the train distribution and so Elliptical Attention is unable to improve performance.

F.2 Representation Collapse

We provide in Figure 6 additional representation collapse results for ImageNet and ADE20K, showing that across modalities Elliptical Attention resists representation collapse.

Table 7: Evaluation of the performance of our model and DeiT across multiple robustness benchmarks, using appropriate evaluation metrics for each.

Dataset	ImageNet-R	ImageNet-A	ImageNet-C	ImageNet-C (Extra)
Metric	Top-1	Top-1	mCE (\downarrow)	mCE (\downarrow)
<i>DeiT</i>	5.77	0.73	72.21	63.68
<i>DeiT-Elliptical</i>	32.66	7.63	73.59	65.71

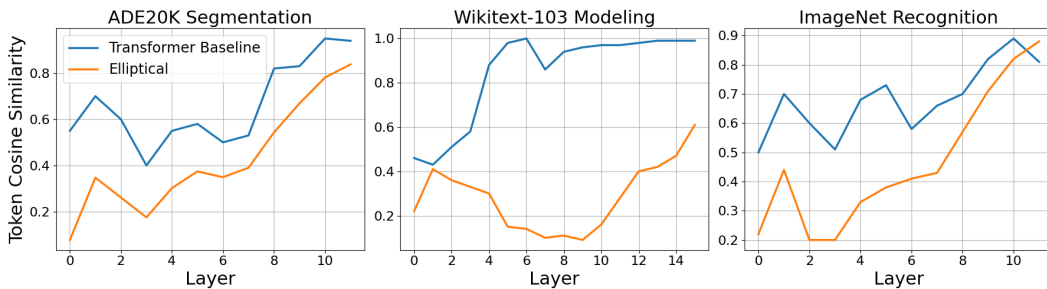


Figure 6: Additional Representation Collapse Results on ADE20K, WikiText-103 and ImageNet. Elliptical reduces token similarity over layers across a range of modalities

F.3 Head Redundancy

We present in Table 9 head redundancy results on the two large-scale tasks, WikiText-103 language modelling and ImageNet-1K object classification. Mean \mathcal{L}_2 distance between vectorized attention heads, with the mean taken over a batch of size 1000 and averaged layer-wise. We see that Elliptical improves head redundancy on WikiText-103 versus the baseline transformer while performing approximately equally to the DeiT baseline on ImageNet.

F.4 Wikitext-103 Language Modelling and Word Swap Attack

Dataset. The WikiText-103 dataset contains around 268K words and its training set consists of about 28K articles with 103M tokens. This corresponds to text blocks of about 3600 words. The validation set and test sets consist of 60 articles with 218K and 246K tokens respectively.

Corruption. Word Swap Text Attack corrupts the data by substituting random words with a generic token 'AAA'.

Model Specification. The small backbone uses 16 layers, 8 heads of dimension 16, a feedforward layer of size 2048, a batch size of 96, and is trained for 120 epochs. The medium backbone uses 16 layers, 8 heads of dimension 32, a batch size of 56, and is trained for 100 epochs.

www.salesforce.com/products/einstein/ai-research/the-wikitext-dependency-language-modeling-dataset/
Implementation available at github.com/QData/TextAttack

Table 8: Additional Results on Imagenet Increasing Heads But Maintaining Overall Embedding Dimension

Model	Num. Heads	Head Dim.	#Params.	Top-1 Accuracy	Top-5 Accuracy
<i>DeiT</i>	3	64	5M	72.23	91.13
<i>Elliptical</i>	3	64	5M	72.36	91.33
<i>DeiT-6head</i>	6	32	5M	72.34	91.22
<i>Elliptical-6head</i>	6	32	5M	73.00	91.77

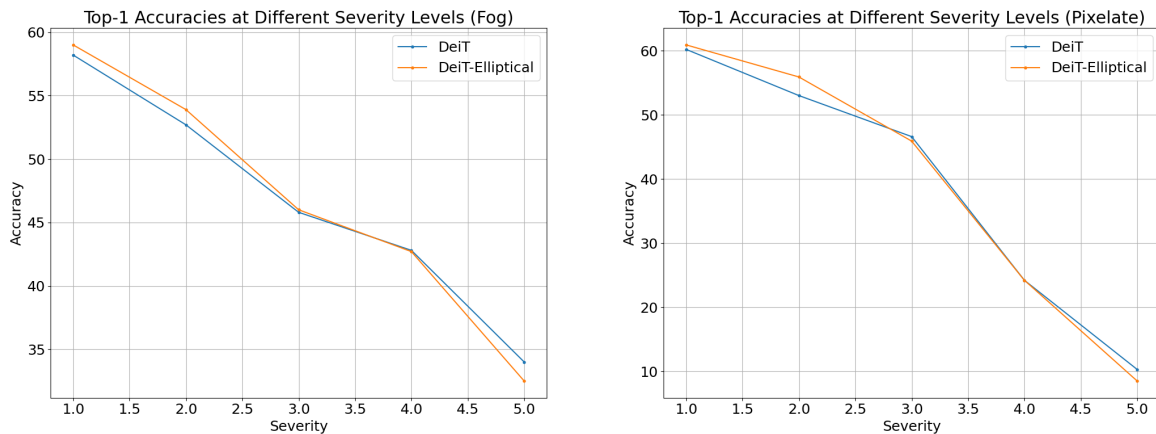


Figure 7: Comparison of *DeiT* versus *DeiT-Elliptical* accuracies on two types of ImageNet-C corruptions, namely, Fog (left) and Pixelate (right). The figures show two out of many cases where *DeiT-Elliptical* outperforms its counterpart while vanilla *DeiT* manages to exceed only at higher severity levels.

For Elliptical Attention, we use an Elliptical layer on all possible layers 1 through 16. We use a constant delta of 1.

Compute Resources. All models are trained and evaluated on two NVIDIA A100 SXM4 40GB GPUs.

F.5 ImageNet Image Classification and Adversarial Attack

Dataset. We use the full ImageNet dataset that contains 1.28M training images and 50K validation images. The model learns to predict the class of the input image among 1000 categories. We report the top-1 and top-5 accuracy on all experiments.

Corruption. We use attacks FGSM [17], PGD [37], and Auto Attack [8] with perturbation budget $1/255$ while SPSA [70] uses a perturbation budget 0.1. All attacks perturb under l_∞ norm. PGD attack uses 20 steps with step size of 0.15.

Table 9: Head Redundancy Results

Model	Num. Heads	Dim. Head	\mathcal{L}_2 Distance
<i>WikiText-103</i>			
<i>Transformer-Small</i>	8	16	5.40 ± 2.21
<i>Elliptical-Small</i>	8	16	6.45 ± 2.38
<i>ImageNet</i>			
<i>DeiT</i>	3	64	5.11 ± 1.67
<i>Elliptical</i>	3	64	4.98 ± 1.54

Model Specification. The configuration follows the default DeiT tiny configuration [68]. This uses 12 layers, 3 heads of dimension 64, patch size 16, feedforward layer of size 768, batch size of 256, and is trained for 300 epochs.

For Elliptical Attention, we use an Elliptical layer on all possible layers 1 through 12. We use a constant delta of 1.

Compute Resources. We train and evaluate all models on four NVIDIA A100 SXM4 40GB GPUs, with the exception of the robustness experiments on ImageNet-C which are conducted using four NVIDIA Tesla V100 SXM2 32GB GPUs.

F.6 LRA Long Sequence Classification.

Dataset. The LRA benchmark consists 5 tasks involving long range contexts of up to 4000 in sequence length. These tasks consist of equation calculation (ListOps) [45], review classification (Text) [36], document retrieval (Retrieval) [52], image classification (Image) [27] and image spatial dependencies (Pathfinder) [32].

Model Specification. The Transformer backbone is set with 2 layers, hidden dimension of 128, 2 attention heads and embedding dimension of 64. Reformer uses 2 hashes, Performer has 256 random feature dimensions and Linformer uses a projection dimension of 256. Elliptical places the Elliptical Attention layer on the final layer (as the only one possible) and uses delta equal to 1.

Compute Resources. All models are trained and evaluated on a single NVIDIA A100 SXM4 40GB GPU.

F.7 ADE20K Image Segmentation

Dataset. ADE20K [77] contains challenging scenes with fine-grained labels and is one of the most challenging semantic segmentation datasets. The training set contains 20,210 images with 150 semantic classes. The validation and test set contain 2,000 and 3,352 images respectively.

Model Specification. The encoder is pretrained on ImageNet for 300 epochs. The encoder configuration follows the default DeiT tiny configuration [68]. This uses 12 layers, 3 heads of dimension 64, patch size 16, feedforward layer of size 768, batch size of 256. The segmenter is then finetuned on ADE20K’s train set for 64 epochs.

Compute Resources. All models are trained and evaluated on a single NVIDIA A100 SXM4 40GB GPU.

F.8 Ablation Studies

Ablation Models. We consider the following models in our ablation studies:

- *Random Ablation.* To validate the efficacy of our proposed estimator given in Eqn. 12, we consider an alternate model in which M is populated by weights uniformly drawn from the $[0, 1]$ interval followed by the same maxscaling as in *Elliptical*.
- *Elliptical-Meanscale.* We ablate the effect of maxscaling by considering meanscaling of the estimates m_i . That is, each $m_i \leftarrow m_i/\bar{m}$ is scaled by the mean variability estimate $\bar{m} = \mathbb{E}_D[m_i]$.
- *Elliptical-Consistent.* We consider also the performance of Elliptical when using the consistent estimator of $\|f'_i\|_{1,\mu}$ described by Equation 51.

Language Modelling. Results are shown in Table 10. Amazingly, the random ablation model performs extremely well on contaminated data. In general, this most likely suggests that training a model with randomness injected into the attention matrix can generate some robustness benefits, which is intuitive. It does, less surprisingly, come at the cost of clean data performance, where Random Ablation performs almost 10% worse than baseline transformer.

ImageNet Classification and Attack. Table 12 shows the ablation model’s performance on both clean ImageNet and under Auto Attack. The ablation model shows a slight improvement over the DeiT baseline in Top 1 accuracy, however Top 5 accuracy is substantially lower. Reasonable performance again Auto Attack is overall unsurprising given that the random Random Ablation model is essentially employing random defence. Nonetheless, it still does not surpass the performance of Elliptical.

Table 10: Perplexity (PPL) of Elliptical and baselines on WikiText-103 under Word Swap data contamination. Best results are in bold. Our Elliptical method achieve substantially better robust PPL without compromising performance on clean data.

Model	Clean Test PPL (\downarrow)	Contaminated Test PPL (\downarrow)
<i>Transformer</i>	34.29	74.56
<i>Performer</i>	33.49	73.48
<i>Transformer-MGK</i>	33.21	71.03
<i>FourierFormer</i>	32.85	68.33
<i>Transformer-SPKDE</i>	32.18	54.97
<i>Transformer-MoM</i>	34.68	52.14
<i>Elliptical</i>	32.00	52.59
<i>Random Ablation</i>	37.84	46.82
<i>Elliptical-Consistent</i>	32.95	54.67
<i>Elliptical-Meanscale</i>	31.94	52.78

Table 11: Evaluation of the performance of our model and DeiT across multiple robustness benchmarks, using appropriate evaluation metrics for each.

Dataset	ImageNet-R	ImageNet-A	ImageNet-C	ImageNet-C (Extra)
Metric	Top-1	Top-1	mCE (\downarrow)	mCE (\downarrow)
<i>DeiT</i>	25.38	3.65	72.21	63.68
<i>Elliptical</i>	31.37	6.76	73.59	65.71
<i>Random Ablation</i>	30.87	5.85	74.02	65.90
<i>Elliptical-Consistent</i>	31.46	6.71	82.92	71.74
<i>Elliptical-Meanscale</i>	32.66	7.63	72.28	63.79

G Broader Impacts

Our research offers benefits to both clean data and robust performance. We in particular show improved results in domains with wide social applicability. These include image segmentation, with benefits to self-driving cars, and language modeling, with benefits to AI chatbot assistants. We in particular show strong improvements against contamination by adversarial attack, which we hope can protect vital AI systems from malicious actors, and competitive performance in contaminated language modeling, which we hope can improve language models evaluated on imperfect data as is often the case in the real world. There is always possibility of misuse of AI systems, however our research shows substantive improvements in fundamental architectures and theory which we hope can spur further socially beneficial outcomes.

Table 12: Auto Attack Ablation Study: Top 1 and Top 5 test accuracies on clean ImageNet and under Auto Attack. The ablation model fails to fit the clean data well and is highly prone to adversarial attack.

Method	<i>DeiT</i> [68]		<i>DeiT-Elliptical</i>		<i>Random Ablation</i>	
	Top 1	Top 5	Top 1	Top 5	Top 1	Top 5
Clean Data	72.23	91.13	72.36	91.33	71.44	91.29
APGD-CE	27.75	66.48	31.27	68.28	27.85	61.74
APGD-T	27.74	73.37	29.69	74.39	28.60	68.72
FAB-T	71.61	90.54	71.74	90.81	68.54	89.43
Square	43.55	80.96	47.25	81.65	47.24	78.87
Average	42.66	77.84	45.00	78.78	43.06	74.69
Sequential Attack	26.08	64.18	27.45	67.77	26.33	60.85

References

- [1] R. Al-Rfou, D. Choe, N. Constant, M. Guo, and L. Jones. Character-level language modeling with deeper self-attention. In *Proceedings of the AAAI conference on artificial intelligence*, volume 33, pages 3159–3166, 2019. (Cited on page 1.)
- [2] A. Baevski and M. Auli. Adaptive input representations for neural language modeling. *arXiv preprint arXiv:1809.10853*, 2018. (Cited on page 1.)
- [3] I. Beltagy, M. E. Peters, and A. Cohan. Longformer: The long-document transformer. *arXiv preprint arXiv:2004.05150*, 2020. (Cited on page 11.)
- [4] L. Chen, K. Lu, A. Rajeswaran, K. Lee, A. Grover, M. Laskin, P. Abbeel, A. Srinivas, and I. Mordatch. Decision transformer: Reinforcement learning via sequence modeling. *Advances in neural information processing systems*, 34:15084–15097, 2021. (Cited on page 1.)
- [5] K. Cho, B. Van Merriënboer, C. Gulcehre, D. Bahdanau, F. Bougares, H. Schwenk, and Y. Bengio. Learning phrase representations using rnn encoder-decoder for statistical machine translation. *arXiv preprint arXiv:1406.1078*, 2014. (Cited on page 1.)
- [6] K. Choromanski, V. Likhoshesterov, D. Dohan, X. Song, A. Gane, T. Sarlos, P. Hawkins, J. Davis, A. Mohiuddin, L. Kaiser, et al. Rethinking attention with performers. *arXiv preprint arXiv:2009.14794*, 2020. (Cited on pages 10 and 11.)
- [7] J. Cohen, E. Rosenfeld, and Z. Kolter. Certified adversarial robustness via randomized smoothing. In K. Chaudhuri and R. Salakhutdinov, editors, *Proceedings of the 36th International Conference on Machine Learning*, volume 97 of *Proceedings of Machine Learning Research*, pages 1310–1320. PMLR, 09–15 Jun 2019. (Cited on page 18.)

- [8] F. Croce and M. Hein. Reliable evaluation of adversarial robustness with an ensemble of diverse parameter-free attacks. In *International conference on machine learning*, pages 2206–2216. PMLR, 2020. (Cited on pages 10 and 28.)
- [9] Z. Dai, Z. Yang, Y. Yang, J. Carbonell, Q. V. Le, and R. Salakhutdinov. Transformer-xl: Attentive language models beyond a fixed-length context. *arXiv preprint arXiv:1901.02860*, 2019. (Cited on page 1.)
- [10] M. Dehghani, S. Gouws, O. Vinyals, J. Uszkoreit, and Ł. Kaiser. Universal transformers. *arXiv preprint arXiv:1807.03819*, 2018. (Cited on page 1.)
- [11] J. Deng, W. Dong, R. Socher, L.-J. Li, K. Li, and L. Fei-Fei. Imagenet: A large-scale hierarchical image database. In *2009 IEEE conference on computer vision and pattern recognition*, pages 248–255. Ieee, 2009. (Cited on page 9.)
- [12] J. Devlin, M.-W. Chang, K. Lee, and K. Toutanova. Bert: Pre-training of deep bidirectional transformers for language understanding. *arXiv preprint arXiv:1810.04805*, 2018. (Cited on page 1.)
- [13] A. Dosovitskiy, L. Beyer, A. Kolesnikov, D. Weissenborn, X. Zhai, T. Unterthiner, M. Dehghani, M. Minderer, G. Heigold, S. Gelly, et al. An image is worth 16x16 words: Transformers for image recognition at scale. *arXiv preprint arXiv:2010.11929*, 2020. (Cited on page 1.)
- [14] C. D. Frost and S. G. Thompson. Correcting for regression dilution bias: comparison of methods for a single predictor variable. *Journal of the Royal Statistical Society: Series A (Statistics in Society)*, 163, 2000. (Cited on page 18.)
- [15] P. Gabbur, M. Bilkhu, and J. Movellan. Probabilistic attention for interactive segmentation. *Advances in Neural Information Processing Systems*, 34:4448–4460, 2021. (Cited on page 12.)
- [16] B. Geshkovski, C. Letrouit, Y. Polyanskiy, and P. Rigollet. The emergence of clusters in self-attention dynamics. In *Thirty-seventh Conference on Neural Information Processing Systems*, 2023. (Cited on page 9.)
- [17] I. J. Goodfellow, J. Shlens, and C. Szegedy. Explaining and harnessing adversarial examples. *arXiv preprint arXiv:1412.6572*, 2014. (Cited on pages 10 and 28.)
- [18] L. Györfi, M. Kohler, A. Krzyzak, H. Walk, et al. *A distribution-free theory of nonparametric regression*, volume 1. Springer, 2002. (Cited on page 5.)
- [19] X. Han, T. Ren, T. Nguyen, K. Nguyen, J. Ghosh, and N. Ho. Designing robust transformers using robust kernel density estimation. *Advances in Neural Information Processing Systems*, 36, 2024. (Cited on pages 1, 10, and 12.)
- [20] M. Janner, Q. Li, and S. Levine. Offline reinforcement learning as one big sequence modeling problem. *Advances in neural information processing systems*, 34:1273–1286, 2021. (Cited on page 1.)

- [21] A. Katharopoulos, A. Vyas, N. Pappas, and F. Fleuret. Transformers are rnns: Fast autoregressive transformers with linear attention. In *International conference on machine learning*, pages 5156–5165. PMLR, 2020. (Cited on page 11.)
- [22] S. Khan, M. Naseer, M. Hayat, S. W. Zamir, F. S. Khan, and M. Shah. Transformers in vision: A survey. *ACM computing surveys (CSUR)*, 54(10s):1–41, 2022. (Cited on page 1.)
- [23] N. Kitaev, Ł. Kaiser, and A. Levskaya. Reformer: The efficient transformer. *arXiv preprint arXiv:2001.04451*, 2020. (Cited on page 11.)
- [24] S. Kpotufe and A. Boularias. Gradient weights help nonparametric regressors. In *Advances in Neural Information Processing Systems*, volume 25, 2012. (Cited on pages 5, 13, and 22.)
- [25] S. Kpotufe, A. Boularias, T. Schultz, and K. Kim. Gradients weights improve regression and classification. *Journal of Machine Learning Research*, 17(22):1–34, 2016. (Cited on pages 5, 13, 22, 23, and 24.)
- [26] D. Kreuzer, D. Beaini, W. Hamilton, V. Létourneau, and P. Tossou. Rethinking graph transformers with spectral attention. *Advances in Neural Information Processing Systems*, 34:21618–21629, 2021. (Cited on page 12.)
- [27] A. Krizhevsky, G. Hinton, et al. Learning multiple layers of features from tiny images. 2009. (Cited on page 29.)
- [28] N. Li, Y. Liu, Y. Wu, S. Liu, S. Zhao, and M. Liu. Robutrans: A robust transformer-based text-to-speech model. In *Proceedings of the AAAI conference on artificial intelligence*, volume 34, pages 8228–8235, 2020. (Cited on page 12.)
- [29] H. Liang, W. Härdle, and R. J. Carroll. Estimation in a semiparametric partially linear errors-in-variables model. *Annals of Statistics*, 27(5):1519–1535, Oct 1999. (Cited on page 18.)
- [30] T. Lin, Y. Wang, X. Liu, and X. Qiu. A survey of transformers. *AI open*, 3:111–132, 2022. (Cited on page 1.)
- [31] Z. Lin, M. Feng, C. N. d. Santos, M. Yu, B. Xiang, B. Zhou, and Y. Bengio. A structured self-attentive sentence embedding. *arXiv preprint arXiv:1703.03130*, 2017. (Cited on page 1.)
- [32] D. Linsley, J. Kim, V. Veerabadran, C. Windolf, and T. Serre. Learning long-range spatial dependencies with horizontal gated recurrent units. *Advances in neural information processing systems*, 31, 2018. (Cited on page 29.)
- [33] J. Liu, T. Singhal, L. T. Blessing, K. L. Wood, and K. H. Lim. Crisisbert: a robust transformer for crisis classification and contextual crisis embedding. In *Proceedings of the 32nd ACM conference on hypertext and social media*, pages 133–141, 2021. (Cited on page 12.)
- [34] Z. Liu, Y. Lin, Y. Cao, H. Hu, Y. Wei, Z. Zhang, S. Lin, and B. Guo. Swin transformer: Hierarchical vision transformer using shifted windows. In *Proceedings of the IEEE/CVF international conference on computer vision*, pages 10012–10022, 2021. (Cited on page 1.)

- [35] Y. Lu, Z. Li, D. He, Z. Sun, B. Dong, T. Qin, L. Wang, and T.-Y. Liu. Understanding and improving transformer from a multi-particle dynamic system point of view. *arXiv preprint arXiv:1906.02762*, 2019. (Cited on pages 9, 11, and 12.)
- [36] A. Maas, R. E. Daly, P. T. Pham, D. Huang, A. Y. Ng, and C. Potts. Learning word vectors for sentiment analysis. In *Proceedings of the 49th annual meeting of the association for computational linguistics: Human language technologies*, pages 142–150, 2011. (Cited on page 29.)
- [37] A. Madry, A. Makelov, L. Schmidt, D. Tsipras, and A. Vladu. Towards deep learning models resistant to adversarial attacks. *arXiv preprint arXiv:1706.06083*, 2017. (Cited on pages 10 and 28.)
- [38] K. Mahmood, R. Mahmood, and M. Van Dijk. On the robustness of vision transformers to adversarial examples. In *Proceedings of the IEEE/CVF international conference on computer vision*, pages 7838–7847, 2021. (Cited on page 12.)
- [39] X. Mao, G. Qi, Y. Chen, X. Li, R. Duan, S. Ye, Y. He, and H. Xue. Towards robust vision transformer. In *Proceedings of the IEEE/CVF conference on Computer Vision and Pattern Recognition*, pages 12042–12051, 2022. (Cited on pages 10 and 12.)
- [40] S. Merity, C. Xiong, J. Bradbury, and R. Socher. Pointer sentinel mixture models. *arXiv preprint arXiv:1609.07843*, 2016. (Cited on page 9.)
- [41] J. Mohapatra, C.-Y. Ko, T.-W. Weng, P.-Y. Chen, S. Liu, and L. Daniel. Higher-order certification for randomized smoothing. *ArXiv*, abs/2010.06651, 2020. (Cited on page 18.)
- [42] J. X. Morris, E. Lifland, J. Y. Yoo, J. Grigsby, D. Jin, and Y. Qi. Textattack: A framework for adversarial attacks, data augmentation, and adversarial training in nlp. *arXiv preprint arXiv:2005.05909*, 2020. (Cited on page 10.)
- [43] E. A. Nadaraya. On estimating regression. *Theory of Probability & Its Applications*, 9(1):141–142, 1964. (Cited on page 3.)
- [44] Y. Nader, L. Sixt, and T. Landgraf. Dnnr: Differential nearest neighbors regression. In *International Conference on Machine Learning*, pages 16296–16317. PMLR, 2022. (Cited on page 13.)
- [45] N. Nangia and S. R. Bowman. Listops: A diagnostic dataset for latent tree learning. *arXiv preprint arXiv:1804.06028*, 2018. (Cited on page 29.)
- [46] T. Nguyen, M. Pham, T. Nguyen, K. Nguyen, S. Osher, and N. Ho. Fourierformer: Transformer meets generalized fourier integral theorem. *Advances in Neural Information Processing Systems*, 35:29319–29335, 2022. (Cited on pages 1, 10, and 12.)
- [47] T. Nguyen, C. A. Uribe, T. M. Nguyen, and R. G. Baraniuk. Pidformer: Transformer meets control theory. *arXiv preprint arXiv:2402.15989*, 2024. (Cited on page 9.)

- [48] T. M. Nguyen, T. M. Nguyen, D. D. Le, D. K. Nguyen, V.-A. Tran, R. Baraniuk, N. Ho, and S. Osher. Improving transformers with probabilistic attention keys. In *International Conference on Machine Learning*, pages 16595–16621. PMLR, 2022. (Cited on pages 10 and 12.)
- [49] Y.-K. Noh, M. Sugiyama, K.-E. Kim, F. Park, and D. D. Lee. Generative local metric learning for kernel regression. *Advances in neural information processing systems*, 30, 2017. (Cited on page 13.)
- [50] Y.-K. Noh, M. Sugiyama, S. Liu, M. C. Plessis, F. C. Park, and D. D. Lee. Bias reduction and metric learning for nearest-neighbor estimation of kullback-leibler divergence. In *Artificial Intelligence and Statistics*, pages 669–677. PMLR, 2014. (Cited on page 13.)
- [51] A. P. Parikh, O. Täckström, D. Das, and J. Uszkoreit. A decomposable attention model for natural language inference. *arXiv preprint arXiv:1606.01933*, 2016. (Cited on page 1.)
- [52] D. R. Radev, P. Muthukrishnan, V. Qazvinian, and A. Abu-Jbara. The acl anthology network corpus. *Language Resources and Evaluation*, 47:919–944, 2013. (Cited on page 29.)
- [53] A. Radford, J. W. Kim, C. Hallacy, A. Ramesh, G. Goh, S. Agarwal, G. Sastry, A. Askell, P. Mishkin, J. Clark, et al. Learning transferable visual models from natural language supervision. In *International conference on machine learning*, pages 8748–8763. PMLR, 2021. (Cited on page 1.)
- [54] A. Radford, K. Narasimhan, T. Salimans, I. Sutskever, et al. Improving language understanding by generative pre-training. 2018. (Cited on page 1.)
- [55] A. Radford, J. Wu, R. Child, D. Luan, D. Amodei, I. Sutskever, et al. Language models are unsupervised multitask learners. *OpenAI blog*, 1(8):9, 2019. (Cited on page 1.)
- [56] C. Raffel, N. Shazeer, A. Roberts, K. Lee, S. Narang, M. Matena, Y. Zhou, W. Li, and P. J. Liu. Exploring the limits of transfer learning with a unified text-to-text transformer. *Journal of machine learning research*, 21(140):1–67, 2020. (Cited on pages 1 and 11.)
- [57] A. Ramesh, M. Pavlov, G. Goh, S. Gray, C. Voss, A. Radford, M. Chen, and I. Sutskever. Zero-shot text-to-image generation. In *International conference on machine learning*, pages 8821–8831. Pmlr, 2021. (Cited on page 1.)
- [58] O. Russakovsky, J. Deng, H. Su, J. Krause, S. Satheesh, S. Ma, Z. Huang, A. Karpathy, A. Khosla, M. Bernstein, et al. Imagenet large scale visual recognition challenge. *International journal of computer vision*, 115:211–252, 2015. (Cited on page 9.)
- [59] M. E. Sander, P. Ablin, M. Blondel, and G. Peyré. Sinkformers: Transformers with doubly stochastic attention. In *International Conference on Artificial Intelligence and Statistics*, pages 3515–3530. PMLR, 2022. (Cited on page 12.)
- [60] J. H. Sepanski, R. Knickerbocker, and R. J. Carroll. A semiparametric correction for attenuation. *Journal of the American Statistical Association*, 89(428):1366–1373, 1994. (Cited on page 18.)

- [61] H. Shi, J. GAO, H. Xu, X. Liang, Z. Li, L. Kong, S. M. S. Lee, and J. Kwok. Revisiting over-smoothing in BERT from the perspective of graph. In *International Conference on Learning Representations*, 2022. (Cited on page 20.)
- [62] C. J. Stone. Optimal global rates of convergence for nonparametric regression. *The annals of statistics*, pages 1040–1053, 1982. (Cited on page 23.)
- [63] B. Tang and D. S. Matteson. Probabilistic transformer for time series analysis. *Advances in Neural Information Processing Systems*, 34:23592–23608, 2021. (Cited on page 12.)
- [64] Q. Tao, F. Tonin, P. Patrinos, and J. A. Suykens. Nonlinear svd with asymmetric kernels: feature learning and asymmetric nyström method. *arXiv preprint arXiv:2306.07040*, 2023. (Cited on page 12.)
- [65] Y. Tay, M. Dehghani, S. Abnar, Y. Shen, D. Bahri, P. Pham, J. Rao, L. Yang, S. Ruder, and D. Metzler. Long range arena: A benchmark for efficient transformers. *arXiv preprint arXiv:2011.04006*, 2020. (Cited on page 9.)
- [66] Y. Tay, M. Dehghani, D. Bahri, and D. Metzler. Efficient transformers: A survey. *ACM Computing Surveys*, 55(6):1–28, 2022. (Cited on page 1.)
- [67] I. Tenney, D. Das, and E. Pavlick. Bert rediscovers the classical nlp pipeline. *arXiv preprint arXiv:1905.05950*, 2019. (Cited on page 1.)
- [68] H. Touvron, M. Cord, M. Douze, F. Massa, A. Sablayrolles, and H. Jégou. Training data-efficient image transformers & distillation through attention. In *International conference on machine learning*, pages 10347–10357. PMLR, 2021. (Cited on pages 1, 10, 11, 12, 29, 30, and 32.)
- [69] Y.-H. H. Tsai, S. Bai, M. Yamada, L.-P. Morency, and R. Salakhutdinov. Transformer dissection: a unified understanding of transformer’s attention via the lens of kernel. *arXiv preprint arXiv:1908.11775*, 2019. (Cited on page 12.)
- [70] J. Uesato, B. O’donoghue, P. Kohli, and A. Oord. Adversarial risk and the dangers of evaluating against weak attacks. In *International Conference on Machine Learning*, pages 5025–5034. PMLR, 2018. (Cited on pages 10 and 28.)
- [71] A. Vaswani, N. Shazeer, N. Parmar, J. Uszkoreit, L. Jones, A. N. Gomez, Ł. Kaiser, and I. Polosukhin. Attention is all you need. *Advances in neural information processing systems*, 30, 2017. (Cited on pages 1, 10, 11, and 12.)
- [72] J. Vig and Y. Belinkov. Analyzing the structure of attention in a transformer language model. *arXiv preprint arXiv:1906.04284*, 2019. (Cited on page 1.)
- [73] K. Q. Weinberger and L. K. Saul. Distance metric learning for large margin nearest neighbor classification. *Journal of machine learning research*, 10(2), 2009. (Cited on page 13.)
- [74] J. Yang, A. Gupta, S. Upadhyay, L. He, R. Goel, and S. Paul. Tableformer: Robust transformer modeling for table-text encoding. *arXiv preprint arXiv:2203.00274*, 2022. (Cited on page 12.)

- [75] S. Zhang and Y. Feng. Modeling concentrated cross-attention for neural machine translation with gaussian mixture model. *arXiv preprint arXiv:2109.05244*, 2021. (Cited on page 12.)
- [76] B. Zhou, H. Zhao, X. Puig, S. Fidler, A. Barriuso, and A. Torralba. Scene parsing through ade20k dataset. In *Proceedings of the IEEE conference on computer vision and pattern recognition*, pages 633–641, 2017. (Cited on page 9.)
- [77] B. Zhou, H. Zhao, X. Puig, T. Xiao, S. Fidler, A. Barriuso, and A. Torralba. Semantic understanding of scenes through the ade20k dataset. *International Journal of Computer Vision*, 127:302–321, 2019. (Cited on page 29.)
- [78] D. Zhou, Z. Yu, E. Xie, C. Xiao, A. Anandkumar, J. Feng, and J. M. Alvarez. Understanding the robustness in vision transformers. In *International Conference on Machine Learning*, pages 27378–27394. PMLR, 2022. (Cited on page 12.)